DEVELOPMENT OF METHODOLOGY FOR DESIGNING WAVE DISK ENGINE BASED ON WAVE DYNAMICS AND THERMODYNAMIC ANALYSIS

By

Dewashish Prashad

A THESIS

Submitted to
Michigan State University
in partial fulfillment of the requirements
for the degree of

Mechanical Engineering--Master of Science

ABSTRACT

DEVELOPMENT OF METHODOLOGY FOR DESIGNING WAVE DISK ENGINE BASED ON WAVE DYNAMICS AND THERMODYNAMIC ANALYSIS

By

Dewashish Prashad

Wave rotor technology is based on pressure wave compression and expansion wave scavenging in a compressible fluid. This can be used to realize compression and exhaust strokes of an IC engine in a rotating disk, power extraction is governed by turbo-machinery principle and constant volume combustion is achieved which makes the wave disk engine a highly fuel efficient devise for power extraction. Wave disk engine primarily consists of a rotor mounted in housing with inlet and outlet ports carved to implement given port timings. As the rotor revolves each channel outlet faces the housing wall for a fraction of revolution until it gets exposed to the outlet port opening in the housing. At high rpm this event is equivalent to sudden opening of valve in a channel filled with pressurized gases, which generates expansion waves. The gases coming out impart angular momentum to the rotor generating power very similar to a reaction turbine operation. As the rotor passes the opening port it faces the housing wall, this event is equivalent to sudden closing of valve which generates hammer shock compressing the air-fuel mixture. When both the ports are closed the spark ignition initiates constant volume combustion resulting in a pressure gain combustion which provides better fuel efficiency. This work focuses on determining the port timings by detailed study of wave dynamics and related thermodynamics of the process. A Methodology is developed using simulation tools to find the desired design.

This work is de lovely brothers F	edicated to my dea Rohit and Shailesh the two years of	and all wonderf	ful friends who	has supported m	Prasad, my e throughout

ACKNOWLEDGEMENTS

I would like to thank Dr. Norbert Mueller, my thesis adviser for his support and inspiration, without his guidance this work wouldn't be possible. Also I want to thank all my peers who worked with me on the wave disk project, there inputs have been critical in every analysis done in this study. I am specially thankful to Dr. Rohitashwa Kiran, my fellow project-mate, who mentored me throughout my study on wave disk engine. Also I want to thank my family and friends (Abhisek Jain, Itishree Swain, Nanda Kumar Sasi, Jessica Mesaros and Anju Kurian) who has given there constant support throughout the period of my Master's degree.

TABLE OF CONTENTS

LIST OF TAB	LES	vii
LIST OF FIGU	RES	ix
KEY TO SYM	BOLS AND ABBREVIATIONS	xii
CHAPTER 1	Introduction	
CHAPTER 2 2.1 2.2	6 · · · · · · · · · · · · · · · · · · ·	4 6 11
2.3	<u>.</u>	11
CHAPTER 3 3.1	Analysis of curved rotor shapes Analysis of Rotor A a) Simulation of Design A of rotor	14 14 16
3.1 3.1	.b) Post Processing of the simulation results.c) Port Timing Calculation	21 25
3.2	 .a) Similar Methodology is applied to this rotor – simulation results .b) Simulations for Rotor B with prescribed ω 	28 29 33
3.4	.a) Chronological Summary of Simulation Comparison of Rotor A, B and C	36 39 41
3.5	.a) DiscussionModified Rotor A.a) Simulation Summary	43 45 47
3.5	b) Chronological Summary of Simulationc) Comparison of Rotor A vs Modified Rotor A	49 51
CHAPTER 4	Conclusion and Future Work	52
REFERENCES	}	53

LIST OF TABLES

Table 1	Quantitative results for the cycle	25
Table 2	RPM	26
Table 3	Time History of the Cycle	26
Table 4	Angular History of the Cycle	26
Table 5	Cycle Summary from Simulations	31
Table 6	Quantitative results for the cycle	31
Table 7	RPM	32
Table 8	Time History of the Cycle	32
Table 9	Angular History of the Cycle	32
Table 10	Quantitative results for the cycle	33
Table 11	Cycle Summary from Simulations	33
Table 12	RPM	34
Table 13	Time History of the Cycle	34
Table 14	Angular History of the Cycle	34
Table 15	Cycle Summary from Simulations	39

Table 16	Quantitative results for the cycle	39
Table 17	RPM	40
Table 18	Time History of the Cycle a	40
Table 19	Angular History of the Cycle	40
Table 20	Comparison of the three rotors	41
Table 21	Cycle Summary from Simulations	49
Table 22	Quantitative results for the cycle	49
Table 23	RPM	50
Table 24	Time History of the Cycle	50
Table 25	Angular History of the Cycle	50

LIST OF FIGURES

Figure 0:	Schematic for Wave disc Engine	1
Figure 1:	Sample image depicting simulation initialization	5
Figure 2:	Schematic of Straight Channel at 7 bar pressure (graph depicts pressure distribution in the channel)	6
Figure 3:	Representation of the Cycle	8
Figure 4:	Diverging Straight Channel	9
Figure 5:	Converging Straight Channel	10
Figure 6:	P-v diagram and T-s diagram	11
Figure 7:	P-v diagram for straight, diverging and converging channel shape	12
Figure 8:	Rotor of WDE, the right side of the figure represent top view.	14
Figure 9:	2D model of single channel of rotor with outer turbine connected with Vane passage, right hand side depicts just the rotor channel meshed for simulations	15
Figure 10:	Simulation Initialization	16
Figure 11:	EVO: Burnt mixture is rushed out (time =0)	18
Figure 12:	Intermidiate Step of the EVO mode (time =.05ms)	18
Figure 13:	The pressure at inlet falls below atmospheric pressure, the inlet port is opened now: IVO (time = .164 ms)	19

Figure 14:	The air-fuel mixture is sucked into the channel, the pressure inside the channel rises up slightly (time = .193 ms)	19
Figure 15:	The outlet port is closed: EVC (time = .455 ms)	20
Figure 16:	The Shockwave reaches the inlet port resulting in precompression (time=.650 ms)	20
Figure 17:	P vs Specific Volume	23
Figure 18:	Torque History	24
Figure 19:	Depiction of Inlet and Outlet angles	27
Figure 20:	3D view for Rotor B	28
Figure 21:	2D Projection for a rotor channel	28
Figure 22:	Sample image durung intermediate time step after exhaust port is opened	29
Figure 23:	P-v diagram and the Torque History	30
Figure 24:	Sample image right before exhaust port is opened	36
Figure 25:	P-v and T-s Diagram	37
Figure 26:	Torque History	38
Figure 27:	Comparison of Rotor A, B and C	41
Figure 28:	Comparison of P-v diagram	42
Figure 29:	Torque-History of all three rotors	43
Figure 30:	Mass-flow-rate at the outlet of the rotors.	44

Figure 31:	3D view of Rotor A- with external row of turbine	45
Figure 32:	Modified Rotor Channel with external channel	46
Figure 33:	Sample image from simulations, depicting pressure contour after the outlet port is opened	47
Figure 34:	P-v ans T-s Diagram	48
Figure 35:	Torque History	48
Figure 36:	Comparitive P-v diagram	51

KEY TO SYMBOLS AND ABBREVATIONS

WDE Wave Disc Engine

EVO Exhaust Valve Open

IVO Inlet Valve Open

EVC Exhaust Valve Closed

L Length of channel

Height of Channel

P Pressure

V Specific Volume

T Temperature

S Specific entopy

We Work done during expansion

Ws Work done during suction of fuel

Q Heat transfer during one cycle

H Cycle efficiency

Wc Work done during compression

t1 (EVO) Time period during EVO

t2 (IVO) Time period during IVO

t3 (EVC) Time period during EVC

t4 (IVC) Time period during IVC

Total Cycle Time

 Θ_1 Angle WDE traverse during EVO

Θ_2	Angle WDE traverse during IVO
Θ_3	Angle WDE traverse during EVC
Θ_4	Angle WDE traverse during precompression step
$\Theta_{ m e}$	Exhaust Angle for WDE
$\Theta_{ m i}$	Inlet Angle of WDE
ω	Angular speed of WDE

CHAPTER 1

Introduction

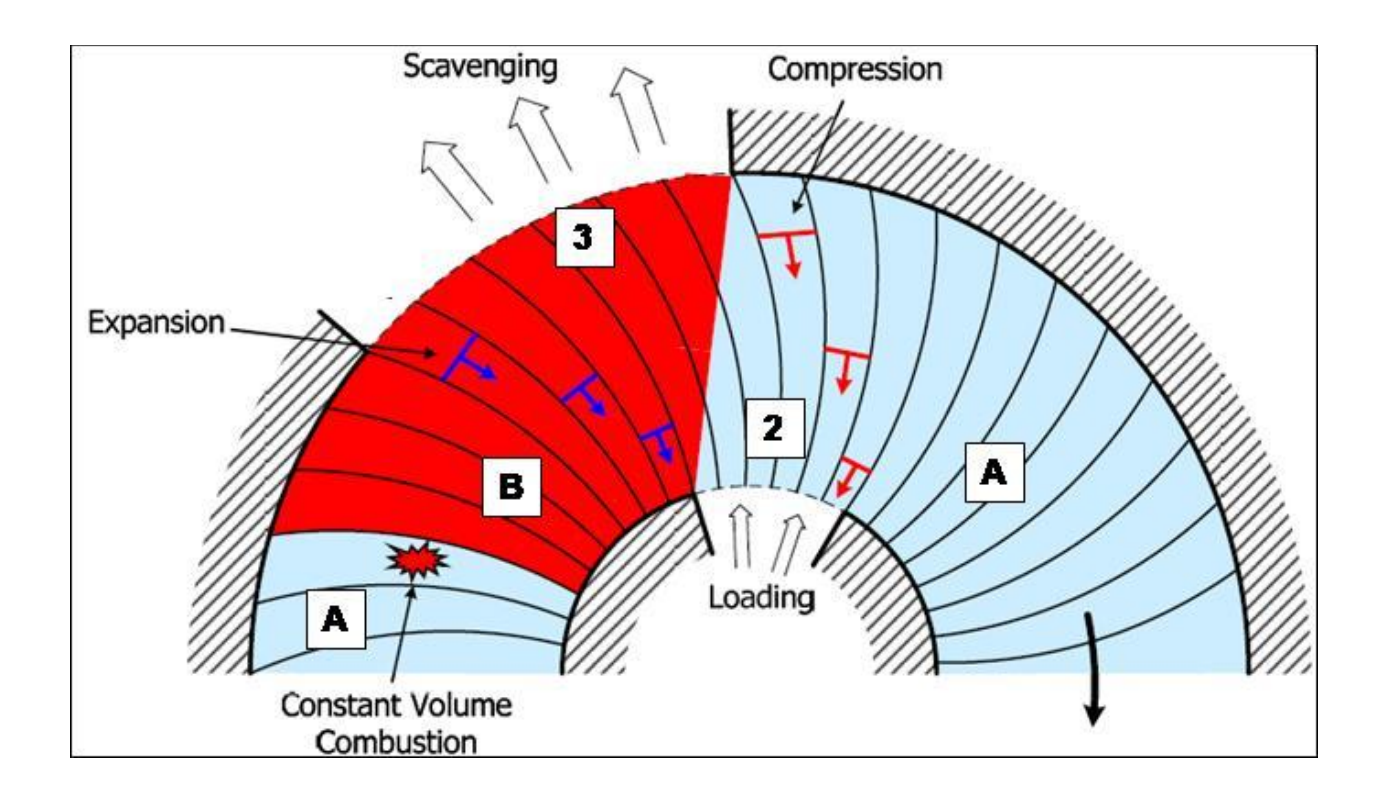


Figure 0: Schematic for Wave disc Engine

Wave disk engine is a novel internal combustion engine [2] which stands apart in terms of fuel efficiency and power to weight ratio in the domain of small scale power output devices. Wave

disk engine utilizes work extraction by reaction turbine mechanism via a rotor revolving in a housing. This is very similar to a gas turbine but the crucial difference is the ability of WDE to achieve pressure gain combustion [3]. There is no external compressor involved for precompression but the hammer shock waves generated by sudden closing of outlet port provides pre-compression for the fresh air-fuel mixture.

Cycle starts right after the combustion ends. The gas inside the rotor channel is at very high pressure and temperature. As the channel revolves to face the exhaust port opening in the stator, the gases starts to rush out generating expansion waves. During this transient channel emptying process, there will be a stage where the channel pressure goes below ambient pressure. At this particular time the inlet port opens up and the fresh air-fuel mixture is sucked in. The gases are still rushing out at the outlet of rotor channel, the order of velocity magnitude is typically 100-200 m/s. As the channel revolves to see the wall at the outlet, a hammer shock is generated as a result of this sudden closing. This compresses the air-fuel mixture. When the compression waves reaches the inlet port, the inlet port closes (channel revolves to face wall at inlet). At this point spark is ignited and combustion begins.

This cycle is referred as Humphrey-Cycle for gas turbines and Atkinson's cycle for IC engine.

When the pre-compression pressure ratio is very low, then the cycle is referred as Lenoir cycle.

The unique features of WDE are its constant volume combustion, compression achieved by shock waves hence no moving element is required and simple physical design which reduces manufacturing cost. Although as the pre-compression is not high therefore WDE belongs to small scale power generation devices.

This work investigates design features for WDE by analyzing 3 different proposed designs of rotors. The heart of design is the estimation of port timing. A methodology is developed to obtain the port timings using numerical simulations using Ansys Fluent commercial package.

The report begins with basic study of wave propagation in straight channel, then based on the inferences three proposed designs are analyzed and optimized design is suggested.

CHAPTER 2

Straight Channel Analysis

Propagation of waves in gases is widely researched phenomenon [1]. As mentioned before, wave dynamics critically affects the determination of port timings [7]. To begin with, propagation of waves in a straight channel is analyzed. Next step would be to investigate effect of change in area or curvature of the channel on the wave propagation. This understanding will be helpful in optimizing channel shape to achieve pre-compression and desired scavenging.

Fluent Simulation start-up details:-

Density based solver is used with inviscid flow model. Roe-Fds scheme is used for discretization with courant number as 1. Explicit formulation for time step is used. Hence the simulation is primarily a marching method in time.

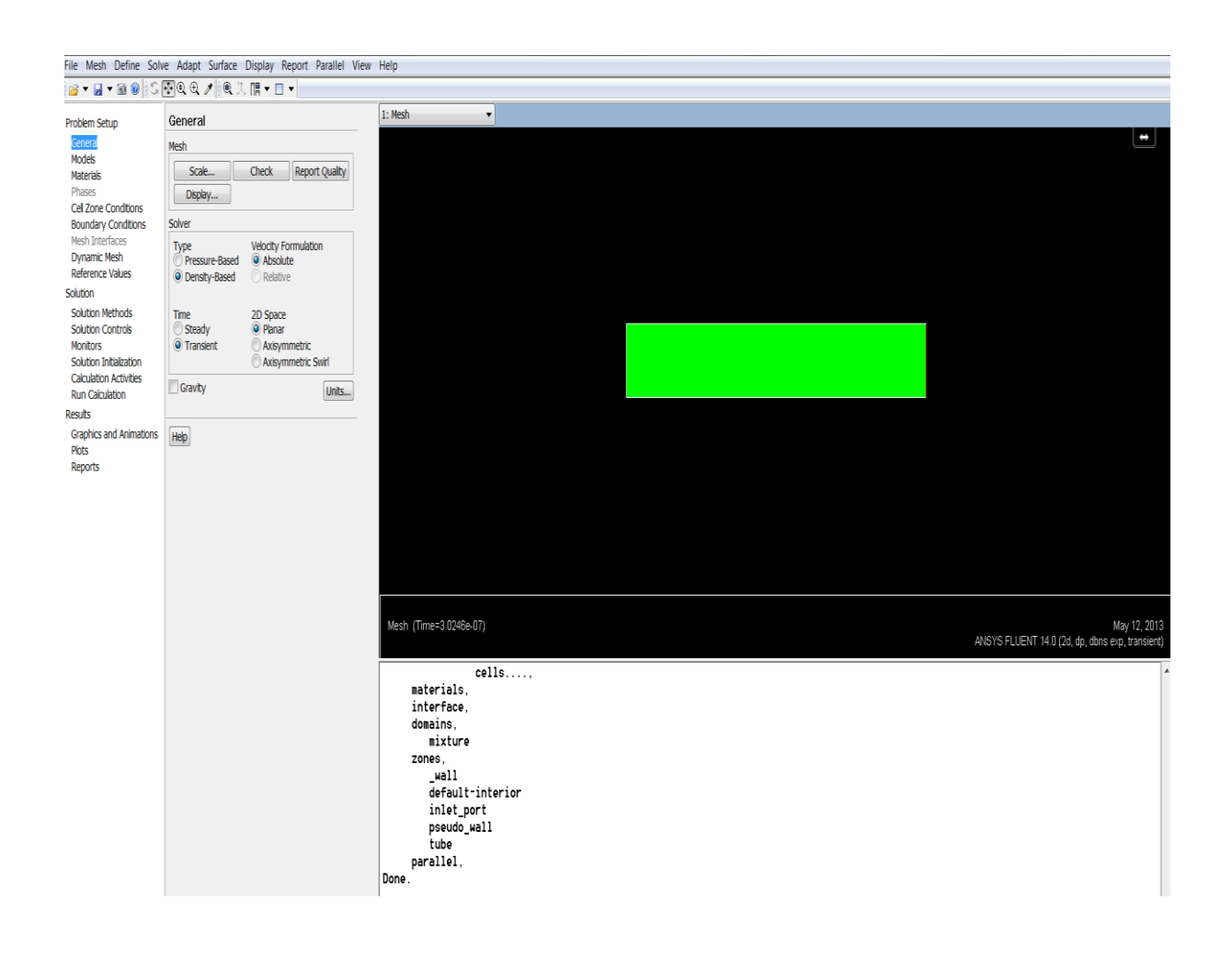


Figure 1: Sample image depicting simulation initialization

2.1 Straight Channel

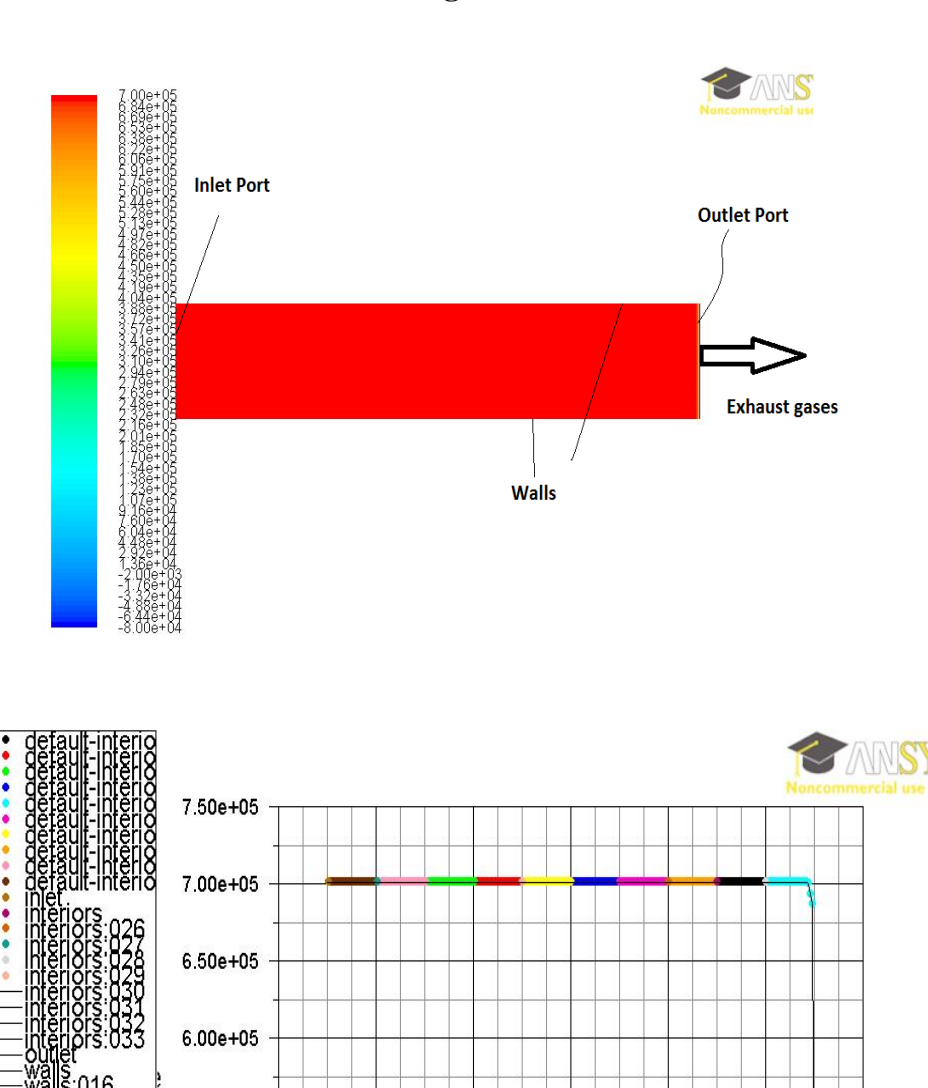


Figure 2: Schematic of Straight Channel at 7 bar pressure (graph depicts pressure distribution in the channel)

0

Position (cm)

2

-2

5.50e+05

5.00e+05

4.50e+05

4.00e+05

The figure 2 represents the straight channel filled with the exhaust mixture (CO2, N2, H2O) at 7 bar. The aspect ratio of channel is $\frac{Length}{Height} = \frac{L}{H} = 5$. The exhaust port or outlet port is opened to atmosphere untill pressure at the inlet port becomes sub-atmospheric, next the inlet port is then opened to take the fresh air-fuel mixture in the channel. When the channel is almost filled the outlet port is closed generating hammer shock wave which compresses air fiel mixture. When the hammer shock reaches the inlet port the inlet port is closed and the mixture is ready for ignition.

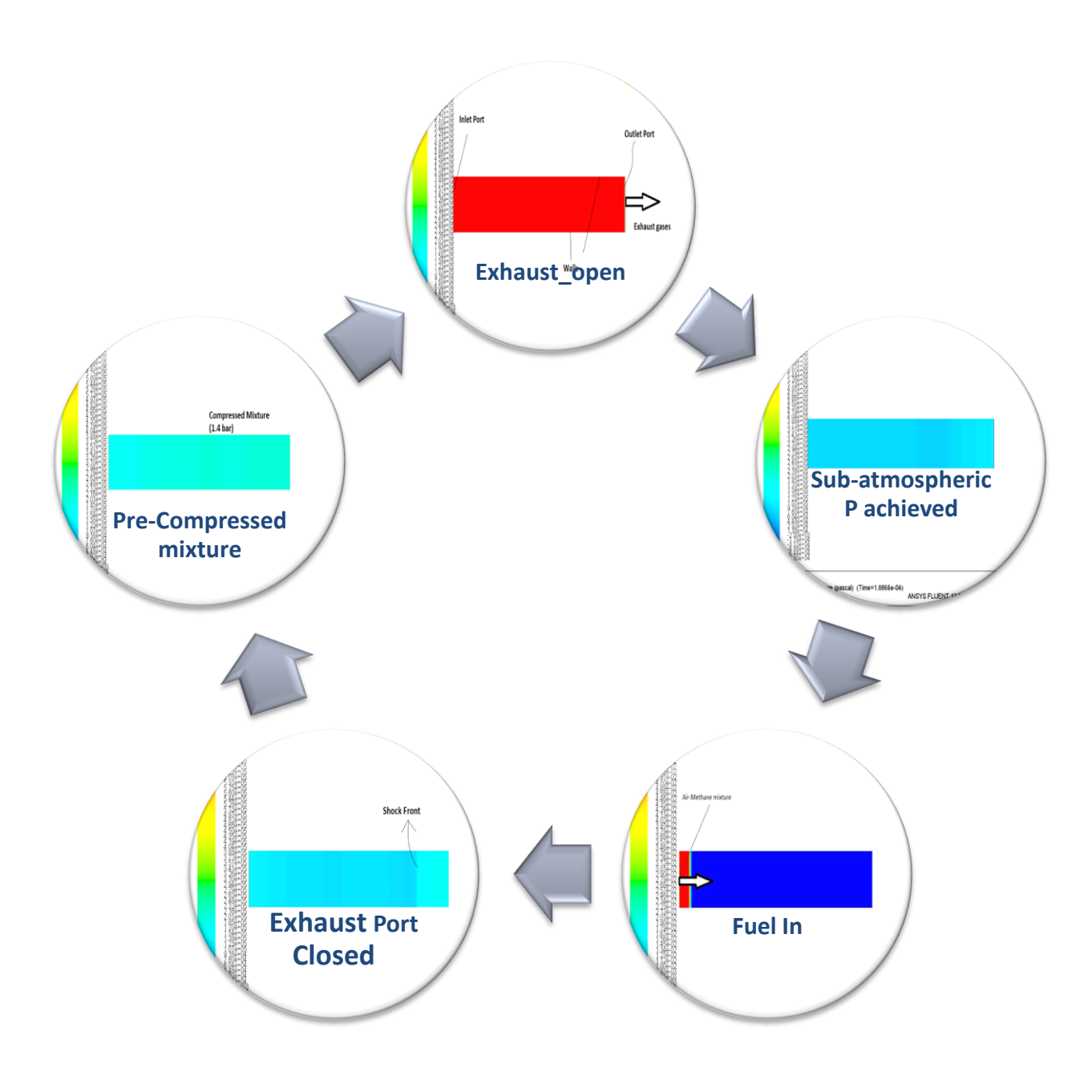


Figure 3: Representation of the Cycle

Similar methodology is repeated for a converging channel and a diverging channel. The notion of converging or diverging channel is used with respect to the hammer shock wave motion.

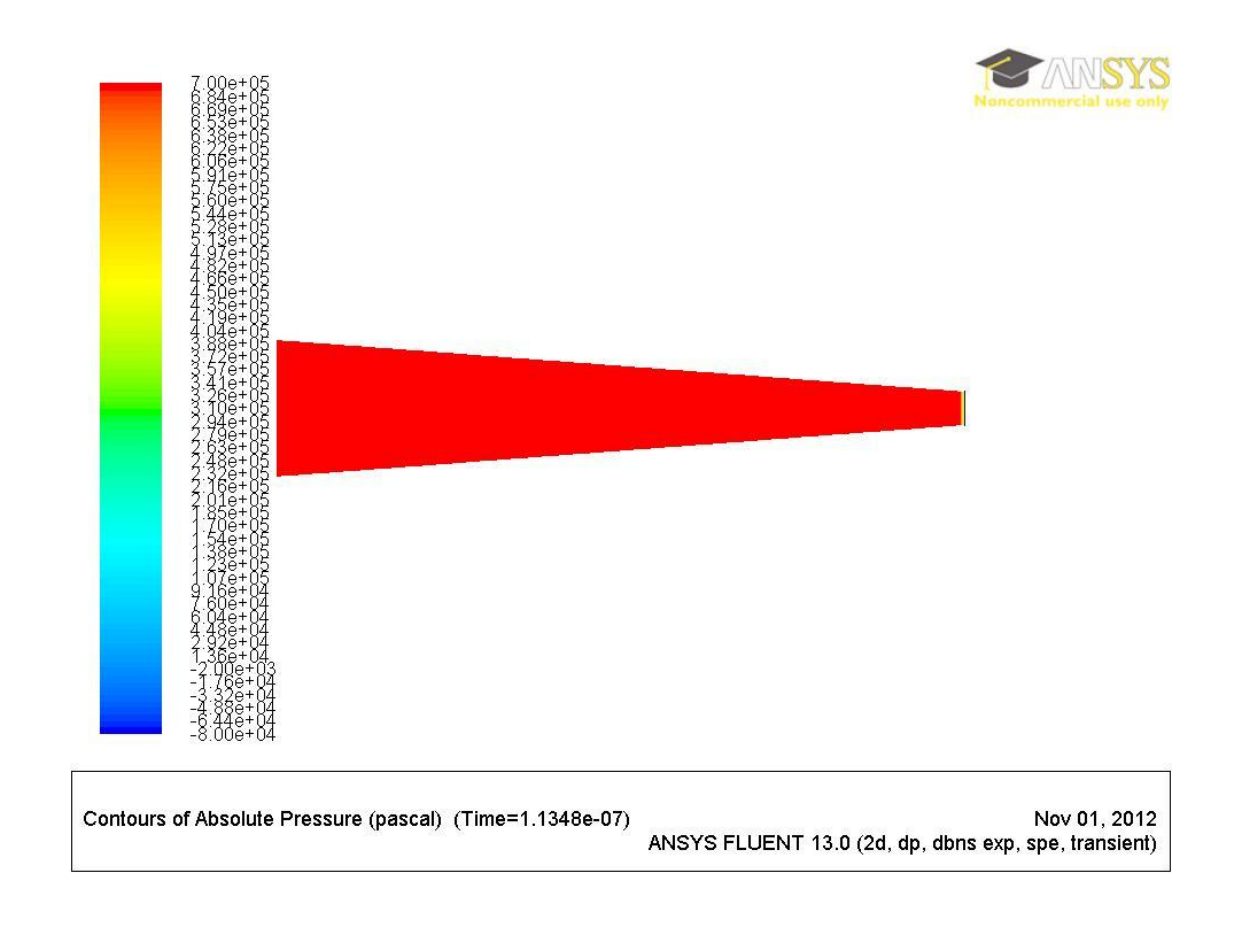


Figure 4: Diverging Straight Channel



Figure 5: Converging Straight Channel

At each time step, the properties of fluid in the chamber: Pressure, Temperature, Density and Entropy is saved. This data is post processed to generate P-v diagrams for the whole cycle. Using these diagrams comparative study is done between various channel shapes simulated.

2.2 Comparision of different channel shapes

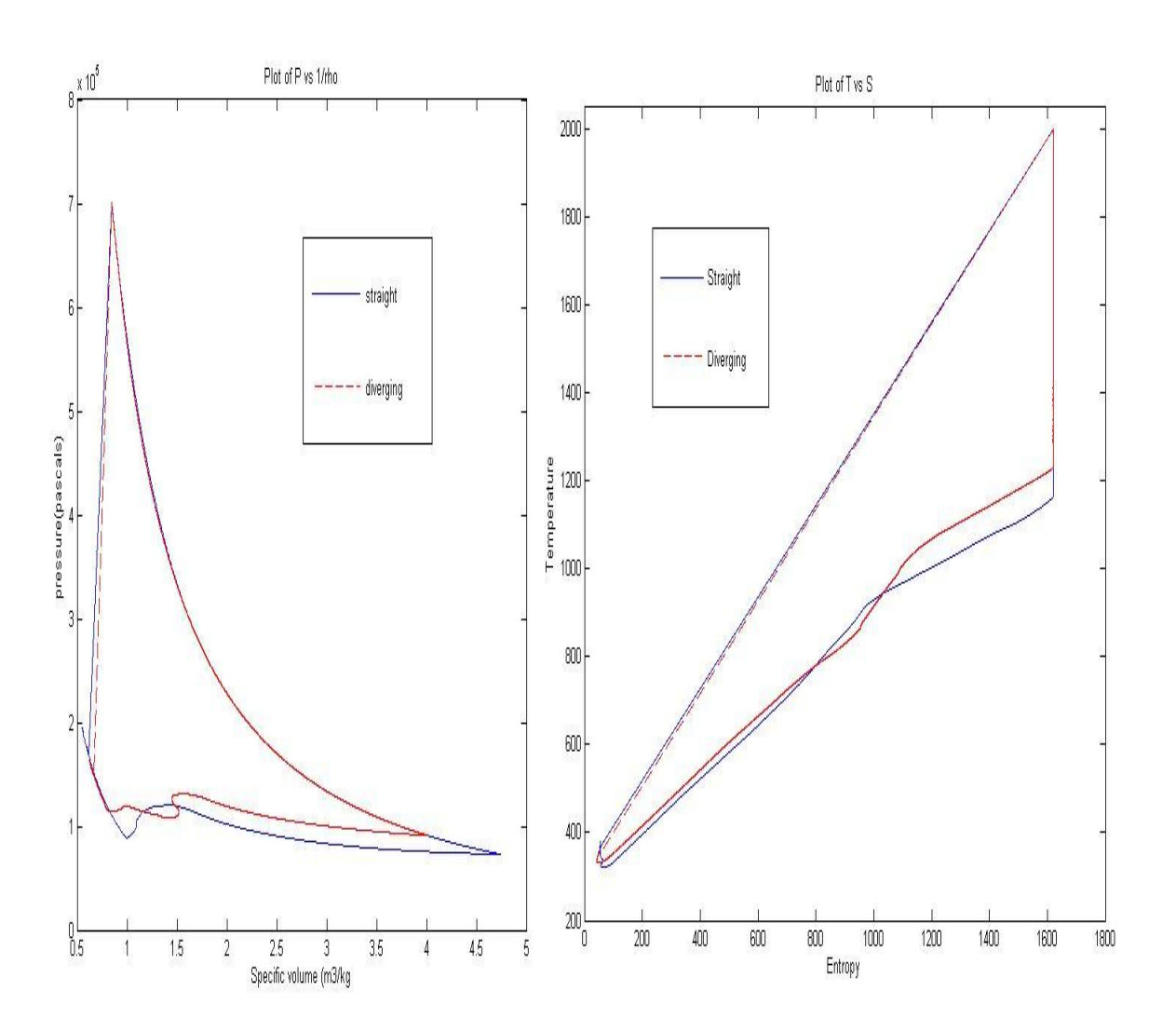


Figure 6: P-v diagram and T-s diagram

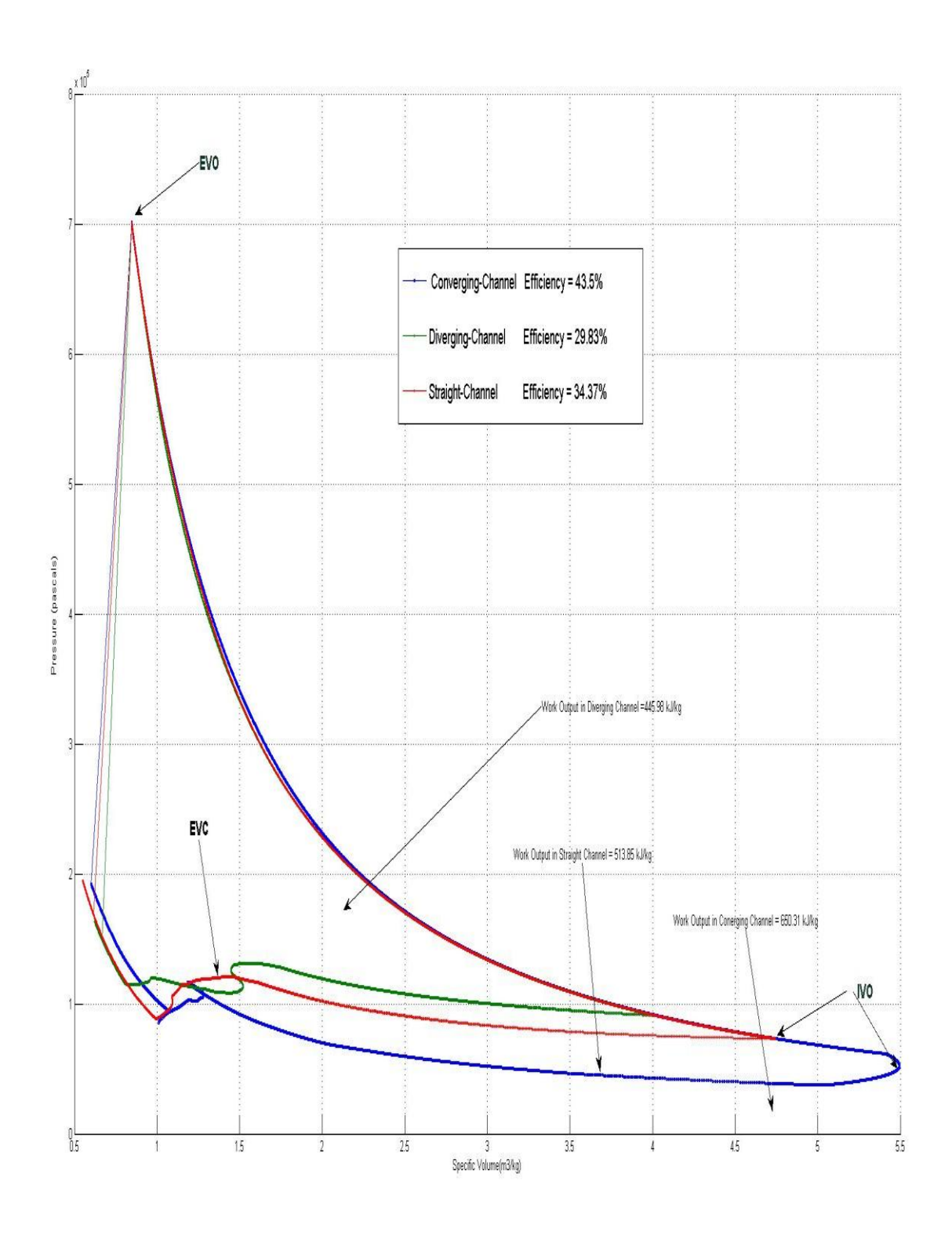


Figure 7: P-v diagram for straight, diverging and converging channel shape

2.3 Discussion

From the straight channel analysis it is clear that compression waves are stronger when they see a converging cross-section, hence the rotor should be designed to utilize this fact. But at the same time a converging cross-section can decrease the strength of expansion waves which can result in low torque output. Hence from this point of view the rotor design is subject to optimization. This will be investigated in later part of this study.

Chapter 3: Analysis of curved rotor shapes

Keeping the results of straight channel in consideration, this chapter will analyse the curved channels and and corresponding rotor efficiency.

3.1 Analysis of Rotor A

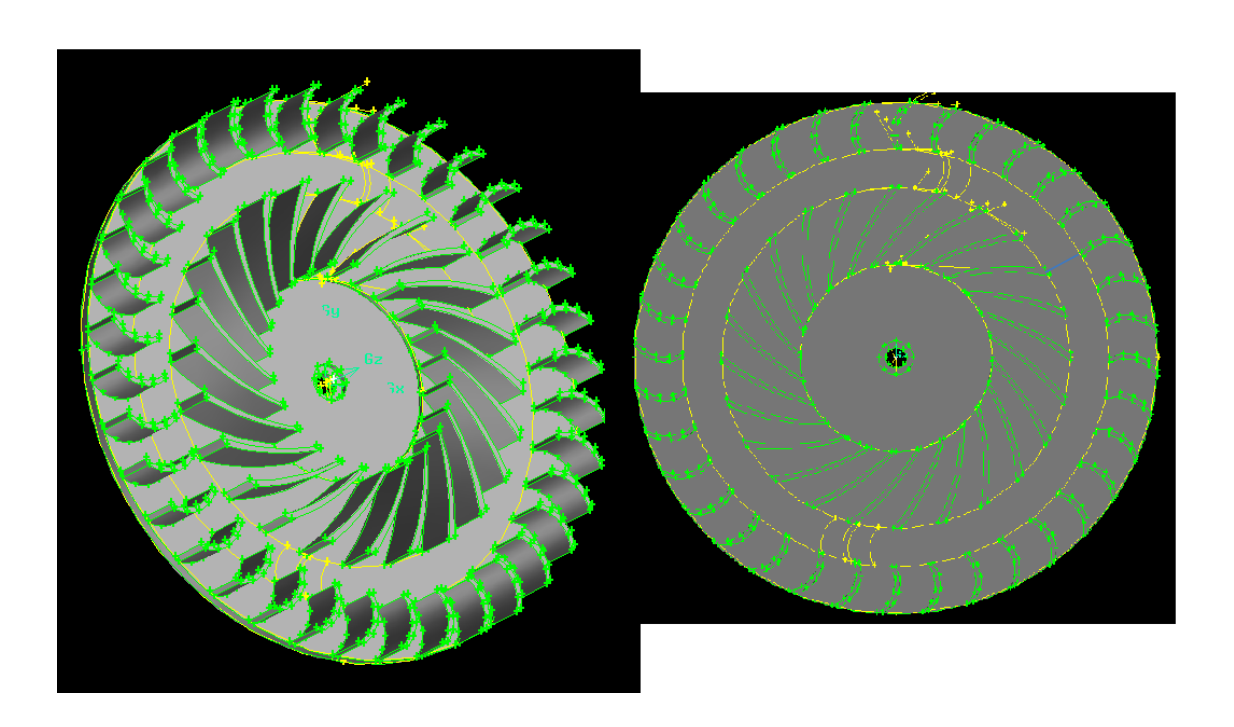


Figure 8: Rotor of WDE, the right side of the figure represent top view.

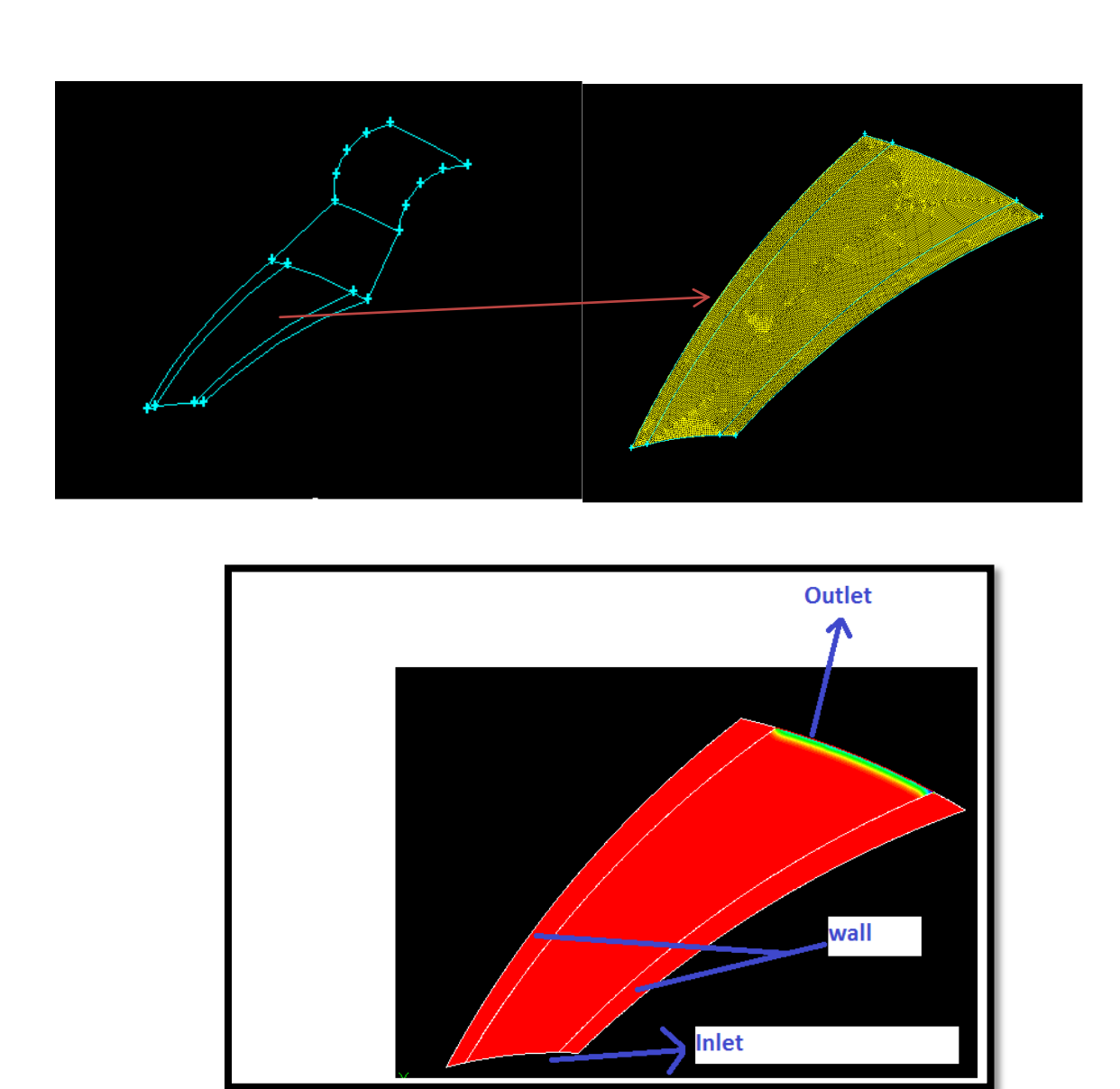


Figure 9: 2D model of single channel of rotor with outer turbine connected with Vane passage, right hand side depicts just the rotor channel meshed for simulations

3.1 a) Simulations for Design A of rotor:

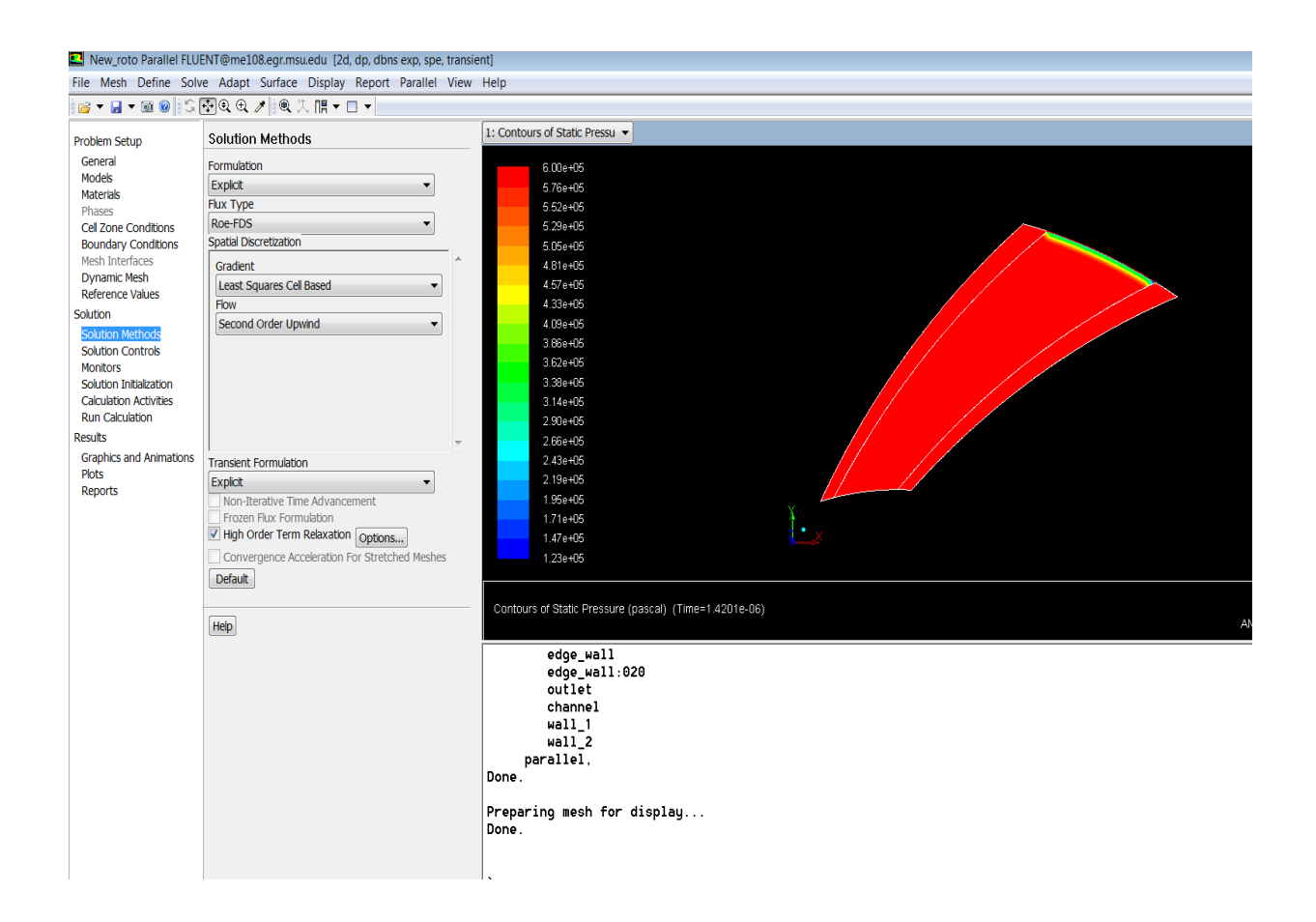


Figure 10: Simulation Initialization

The figure above is the depiction of how the simulation is initialized. Inviscid, density based model in Ansys Fluent is used to simulate the wave phenomenon in the channel. ROE-FDS Explicit[1]. Scheme is used with explicit transiient formulation. Mesh size is ¼ mm.

The channel is initialized with 7 bar pressure and 2000K temperature which is chosen to emulate post combustion properties of system.

Simulation has three broad divisions:

- 1) **EVO** (exhaust valve opens): Outlet boundary condition is set as "Pressure Outlet" (1 atm), inlet port is kept as "wall".
- 2) **IVO** (inlet valve closed): Inlet port is opened to get the fuel in. inlet boundary condition is set to "Pressure inlet" with 1.2 bar of air-fuel mixture pressure and 300K temperature. The Exhaust port is still open.
- 3) **EVC** (exhaust valve closes): The exhaust port or outlet port is closed while the inlet port is still opened.

As the solution is intialized and it marches in time, depending on the pressure of the channel the boundary conditions are changed manually to switch EVO mode to IVO and finally into EVC.

The idea is when solution starts in EVO mode ie when the outlet port opens and expansion waves decreases the pressure of the channel, the inlet port should be opened when the pressure goes sub atmospheric level. This result in suction of fuel which is at higher pressure(1.2 bar, assuming turbocharging or supercharging). Contours of CH4 are tracked to monitor how much fuel has entered, when the channel is almost filled the outlet port is closed ie the outlet boundary condition is switched from "pressure outlet" to "wall". This result in generation of hammer shock wave which compresses the incoming air-fuel charge. When the shock wave reaches inlet

of the channel, the simulation is stopped. The pre-combustion stage is achieved. This methodology is represented in the following contour diagrams and pressure plots.

The left image is the pressure plot and the right image is pressure contour.

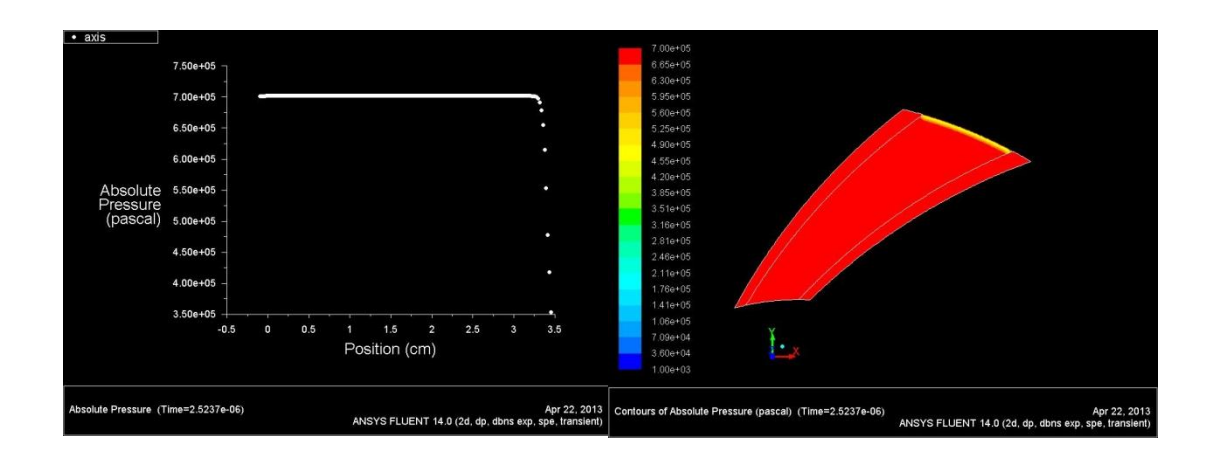


Figure 11 EVO: Burnt mixture is rushed out (time =0)

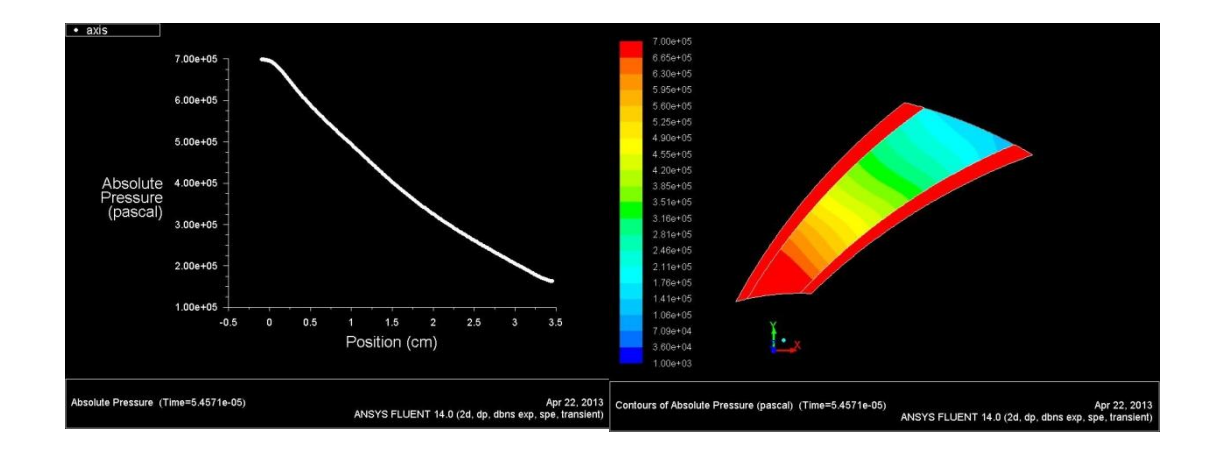


Figure 12 Intermidiate Step of the EVO mode (time =.05ms)

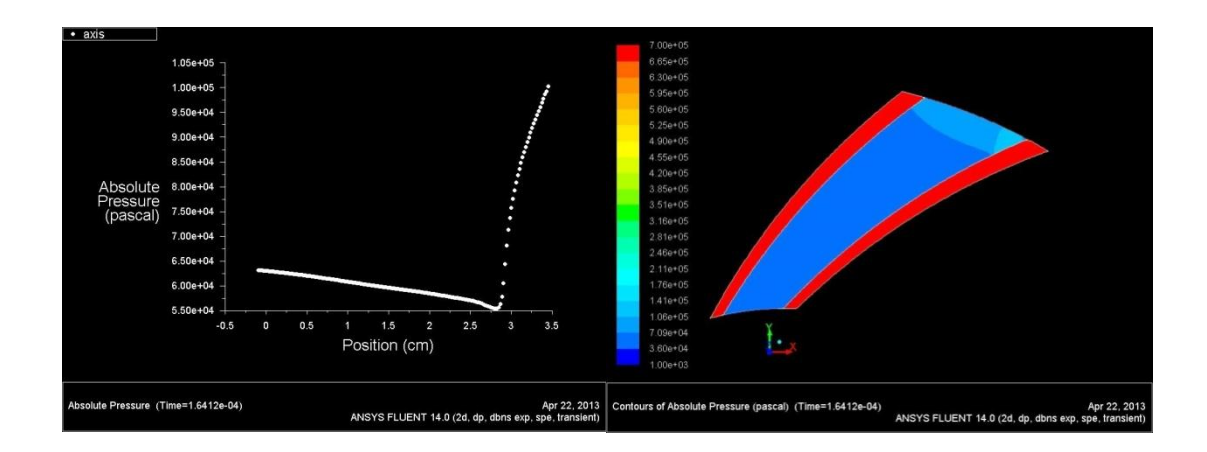


Figure 13 The pressure at inlet falls below atmospheric pressure, the inlet port is opened now:

IVO (time
$$= .164 \text{ ms}$$
)

Right hand side of image below represents the mole fraction contours of methane, the blue color represents burnt gases.

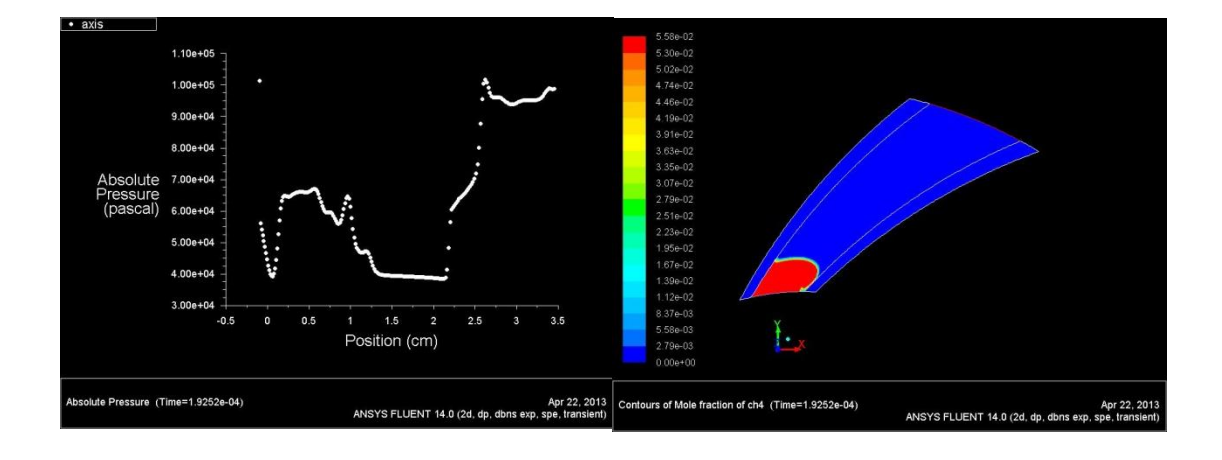


Figure 14 The air-fuel mixture is sucked into the channel, the pressure inside the channel rises up slightly (time = .193 ms)

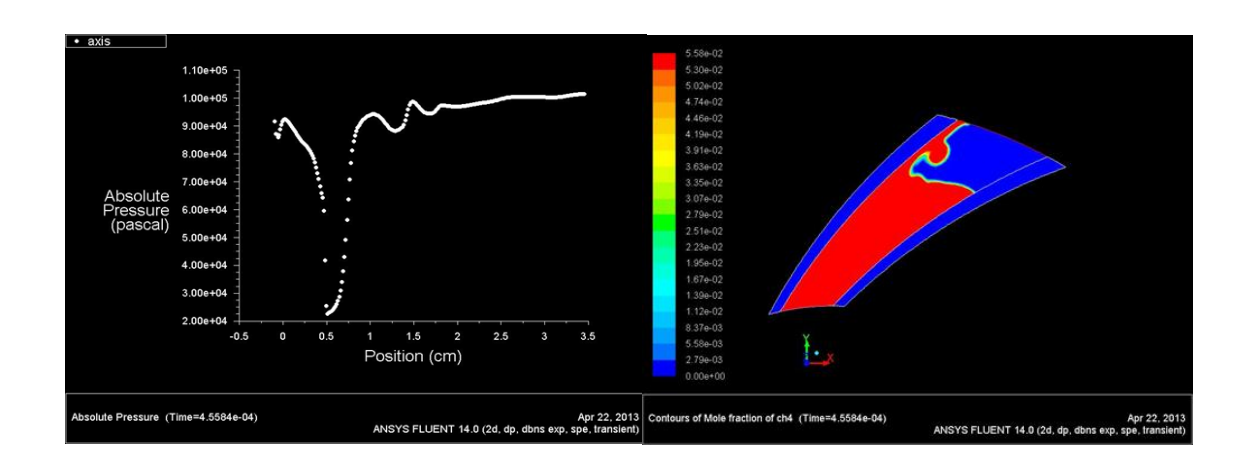


Figure 15 The outlet port is closed : EVC (time = .455 ms)

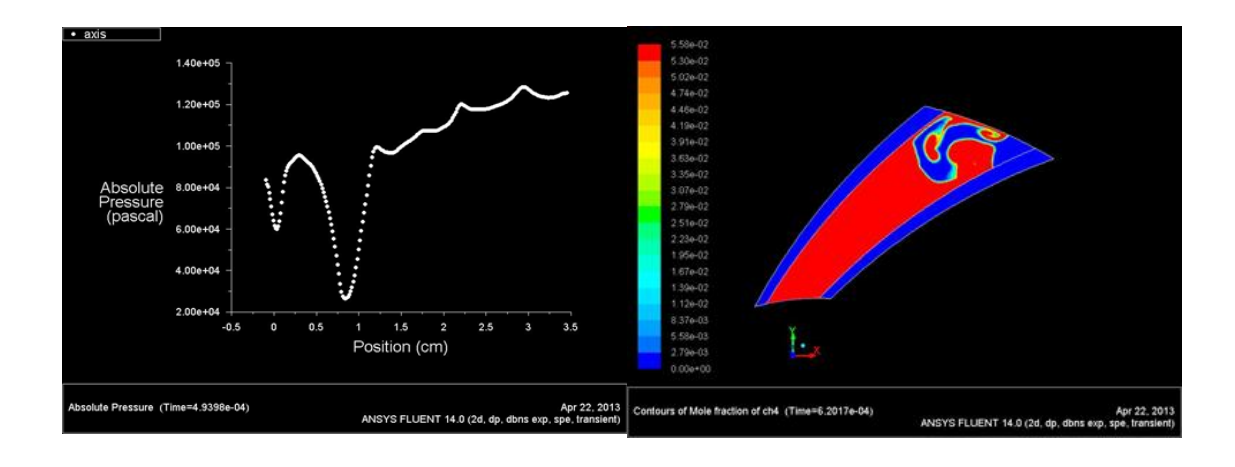


Figure 16 The Shockwave reaches the inlet port resulting in precompression (time=.650 ms)

3.1 b) Post Processing of the simulation results

The work done by the gasses coming out from the channel is governed by unsteady flow physics. To calculate the work done in each mode (EVO, IVO,EVC) the first law of thermodynamics is used as applied to a control volume considering all transient terms.

$$\frac{dE_{CV}}{dt} = \dot{Q} + \dot{m}_{in}h_{tot,in} - \dot{m}_{out}h_{tot,out} - \dot{W}$$

This equation is integrated over time to find the workdone during exhaust stroke, compression stroke and the fuel suction stroke. This is work done by the gases hence the positive sign of W will indicate work output and negative sign will indicate work input.

$$W_{c} = \int_{t_{1}}^{t_{2}} \dot{m}_{in} h_{tot,in} dt - \int_{t_{1}}^{t_{2}} \frac{dE_{CV}}{dt} dt$$
$$= \int_{t_{1}}^{t_{2}} \dot{m}_{in} h_{tot,in} dt + E_{1} - E_{2}$$

$$W_{e} = -\int_{t_{3}}^{t_{4}} \dot{m}_{out} h_{tot,out} dt - \int_{t_{3}}^{t_{4}} \frac{dE_{CV}}{dt} dt$$
$$= -\int_{t_{3}}^{t_{4}} \dot{m}_{out} h_{tot,out} dt + E_{3} - E_{4}$$

$$W_{s} = \int_{t_{4}}^{t_{5}} \dot{m}_{in} h_{tot,in} dt - \int_{t_{4}}^{t_{5}} \dot{m}_{out} h_{tot,out} dt - \int_{t_{4}}^{t_{5}} \frac{dE_{CV}}{dt} dt$$
$$= \int_{t_{4}}^{t_{5}} \dot{m}_{in} h_{tot,in} dt - \int_{t_{4}}^{t_{5}} \dot{m}_{out} h_{tot,out} dt + E_{4} - E_{5}$$

where $E_1 = E_5$ due to the periodicity.

Adding all three expressions of the work done by the fluid, we obtain

$$W_{net} = W_c + W_e + W_s$$

Wc, We, and Ws represent the work done during compression (EVC), exhaust(EVO) and fuel suction(IVO) stages.

To use above equations we need the properties of the flow at each time step. Therefore pressure, density, entropy, temperature, mass flow rate, enthalpy, and total energy of the gases inside the channel is averaged over entire volume and at required surface areas of control volume at each time step. This data is then used estimate the work done by the gases and constructing cycle diagrams.

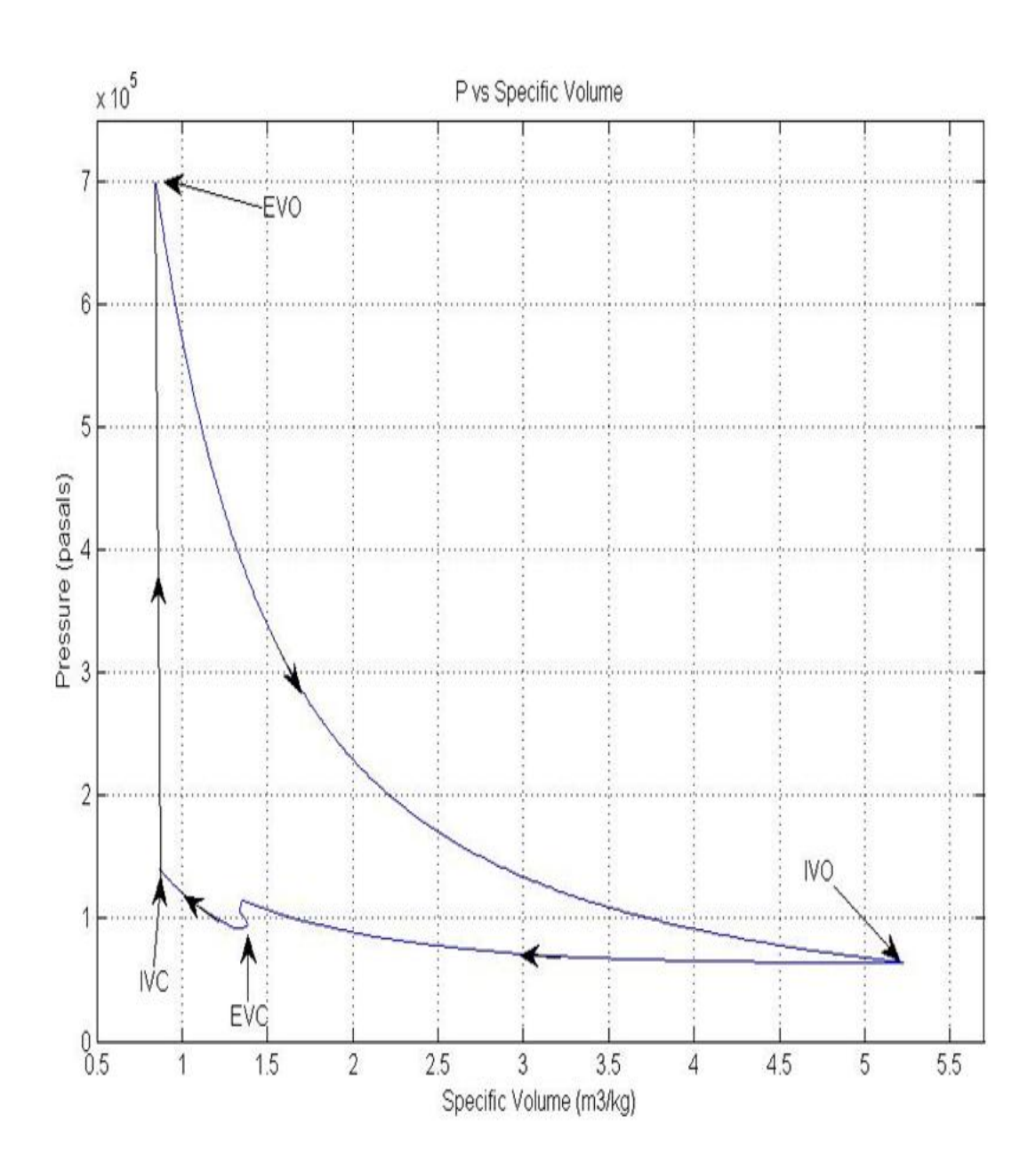


Figure 17: P vs Specific Volume

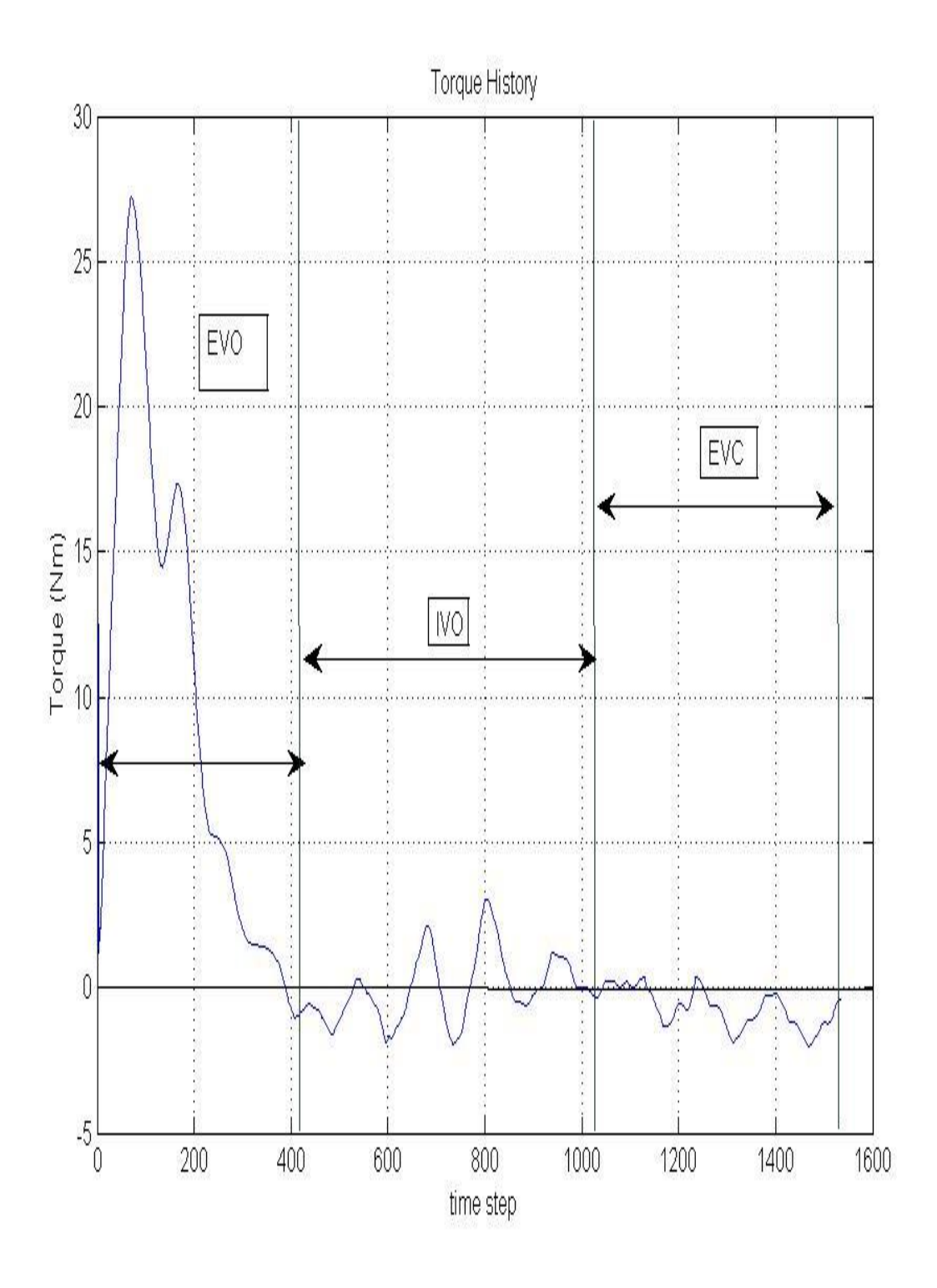


Figure 18: Torque History

The P-v (specific volume) is constructed by using average pressure and density values of channel at each time step. Similarly torque history is recorded at each time step. As clear from the graph the torque output is an impulse acting over the channel. The peak of the impulse is governed by the channel shape and port timings. The quantitative results for the cycle are summarized below:

Table 1: Quantitative results for the cycle

Wc	-79.34 J
We	379.65 J
Ws	24.56 J
Q	949.2 J
Н	34.25 %

3.1 c) Port Timing Calculation

The port timing can be calculated if the rotational velocity (ω) of rotor is known. The ω can be calculate dusing the energy balance for complete cycle. What is the net work output of the cycle.

This value must be equal to the expression:-

$$\int_{0}^{\theta} \tau d\theta = \int_{0}^{T} \tau \omega dt = \omega \int_{0}^{T} \tau dt$$

= work done during one cycle over time interval T

or, Wnet =
$$\omega \int_0^T \tau dt$$

$$\omega = \text{Wnet} / \int_0^T \tau dt$$

Whet is calculated above and integral of torque (τ) over interval T can be calculated as the torque history over time is known. This gives ω =

Table 2: RPM

Ω	17000 rpm
	1780.24 rad/s

Table 3 : Time History of the Cycle

t1 (EVO)	1.5 ms	7bar to below 1bar
t2 (IVO)	0.9 ms	fuel in
t3 (EVC)	0.85 ms	pre compression
t4 (IVC)	3.53 ms	Combustion
Т	7 ms	time period

Table 4 : Angular History of the Cycle

$\Theta_1 = \omega \times t1$	153 deg	Exhaust Angle
$\Theta_2 = \omega \times t2$	91.8 deg	$\Theta_e = \Theta_1 + \Theta_2 =$
		244.8 deg
$\Theta_3 = \omega \times t3$	86.7 deg	Inlet Angle
$\Theta_4 = \omega \times t4$	360 deg	$\Theta_{\rm i} = \Theta_2 + \Theta_3$
		=178.5 deg

The angular sizing of the ports is determined on the basis of the time intervals t1, t2, t3, and t4 which are governed by the result of numerical simulations. These values implicitly depends on the aspect ratio chosen for the given channel. For rotor A aspect ratio Length / width = 5. With radial length of the channel is 5 cm. Because of very high rpm requirement owing to low torque output, the combustion should be timed such that ignition should start in next cycle, this implies there is 1 power stroke in 2 revolution, one complete revolution is used for combustion. Hence using the described approach rpm and exact required size of the rotor can be determined.

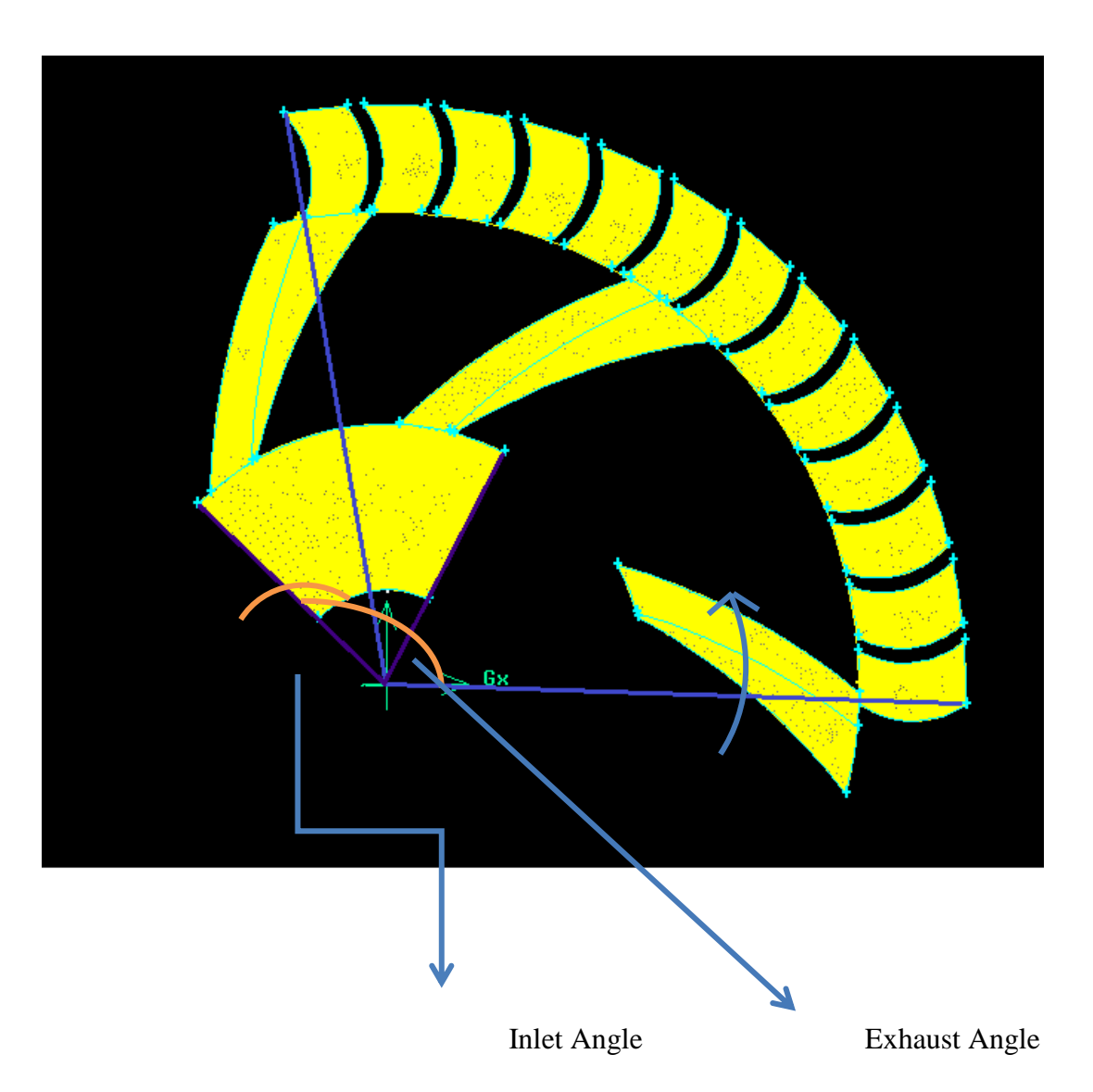


Figure 19: Depiction of Inlet and Outlet angles

3.2 Analysis of Rotor B

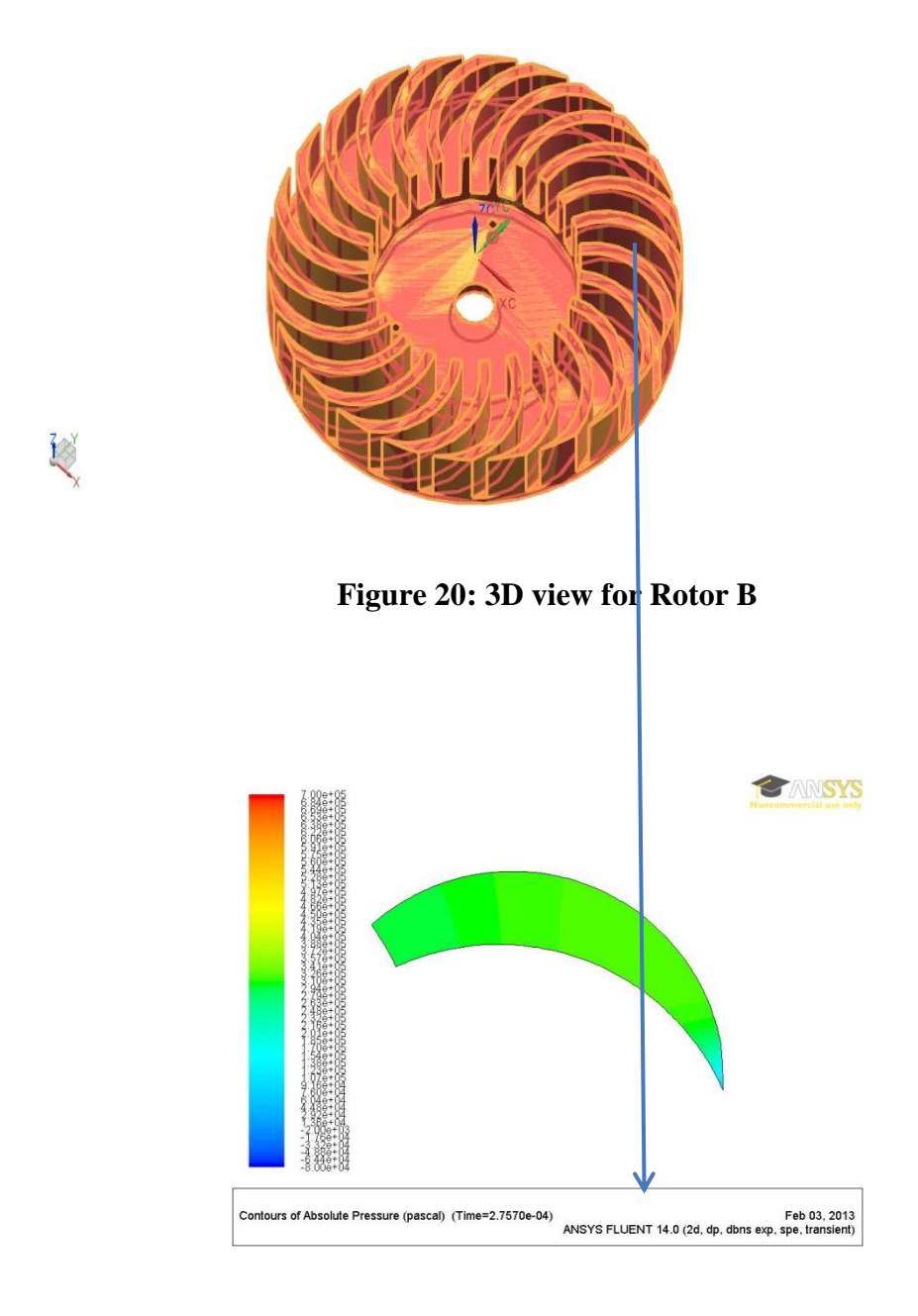


Figure 21: 2D Projection for a rotor channel

3.2 a) Similar Methodology is Applied to this rotor – simulation results

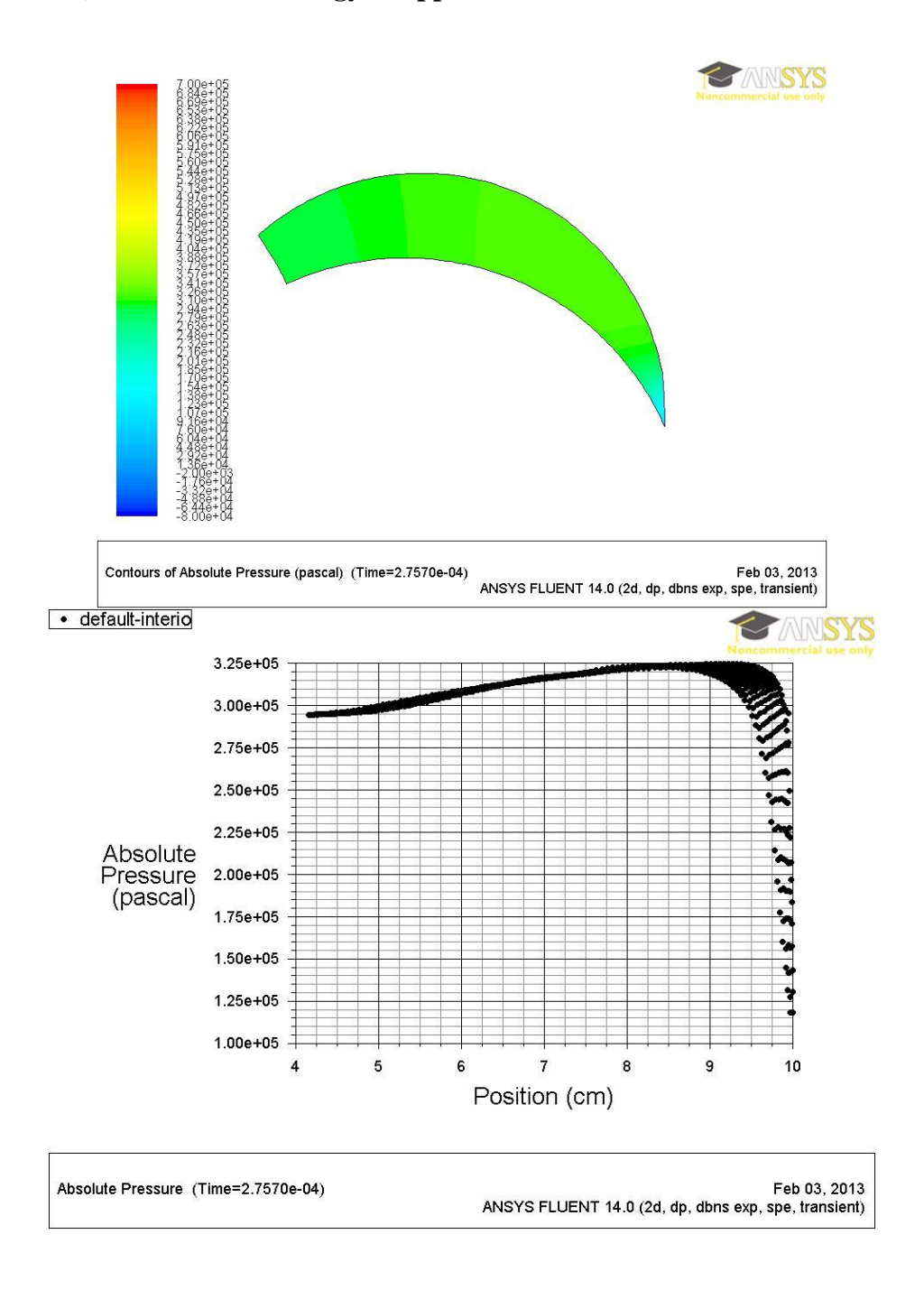
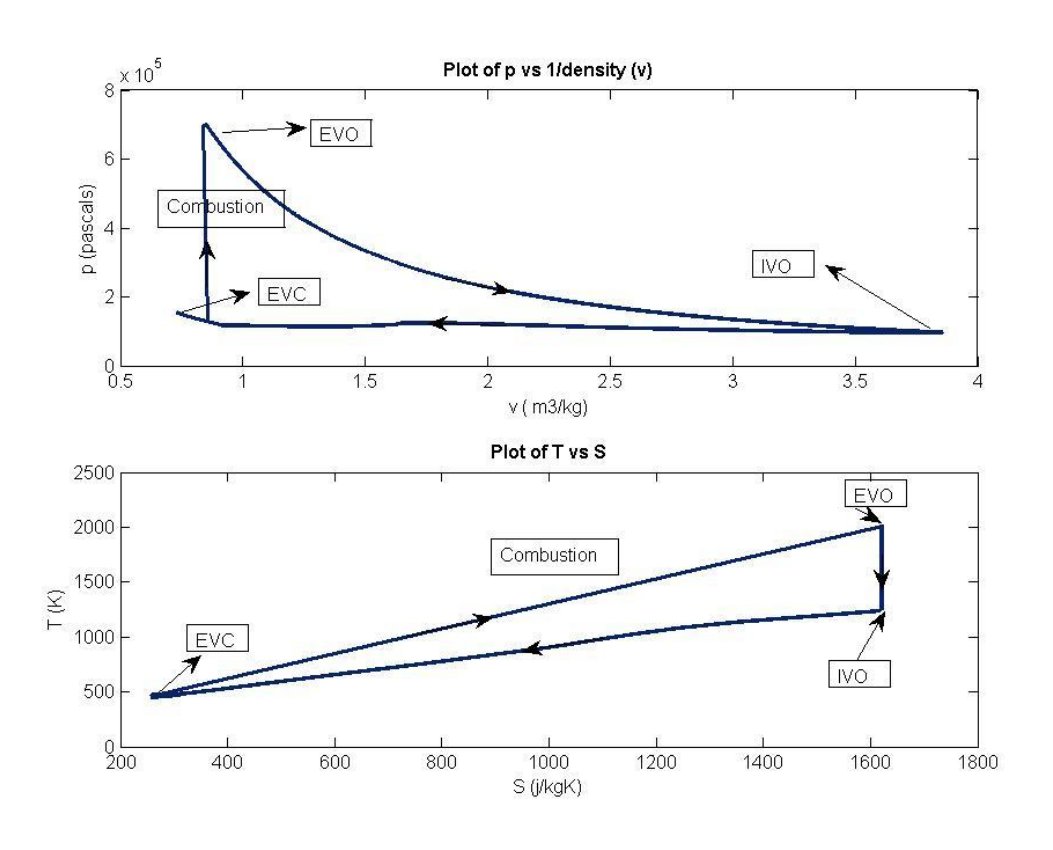


Figure 22: Sample image durung intermediate time step after exhaust port is opened



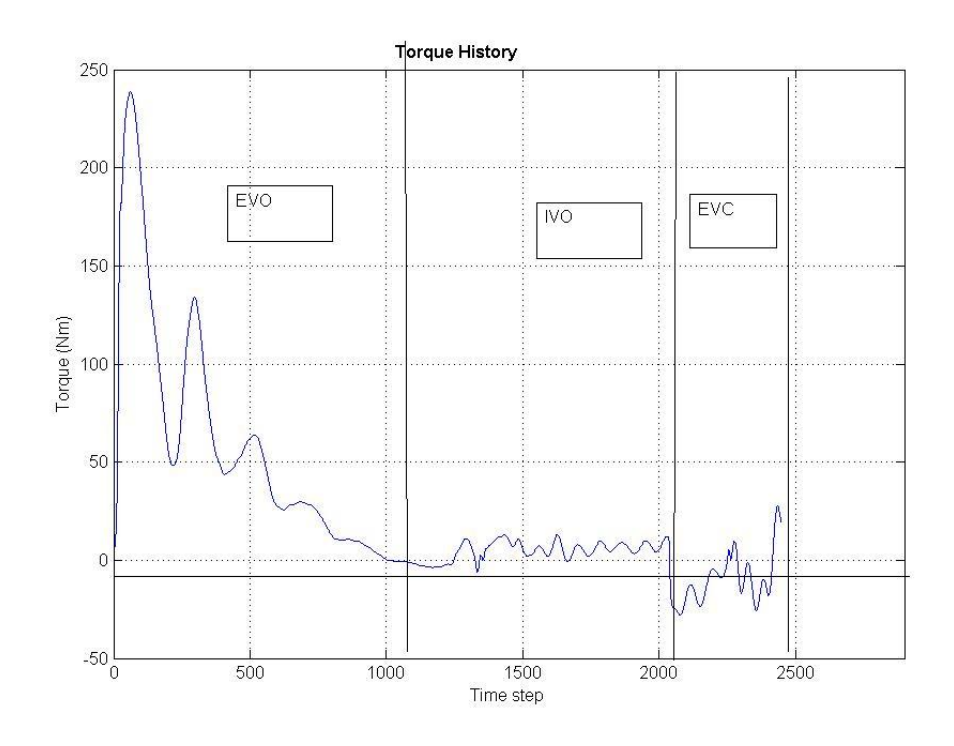


Figure 23: P-v diagram and the Torque History

3.2 b) Chronological Summary of Simulation

Table 5 : Cycle Summary from simulations

Mode (port-setting)	Time	Iteration number	Average P and T
Intialization	0	0	7 bar, 2000K
EVO	0	0	7 bar, 2000K
IVO	.91 ms	12204	.9 bar, 1200 K
EVC	1.65 ms	212204	1.2 bar, 481.7 K
Ignition	1.87 ms	23991	1.55 bar, 471 K

Table 6 : Quantitative results for the cycle

Wc	17.55 J
We	587.54 J
Ws	3.35 J
Q	1.108 kJ
Н	54.45 %

As calculated above the rotational speed is determinjed as :-

$$\omega = \operatorname{Wnet} / \int_0^T \tau dt$$

Table 7: RPM

Ω	10,963 rpm
	1148 rad/s

Table 8 : Time History of the Cycle

t1 (EVO)	.91 ms	7bar to below 1bar
t2 (IVO)	.74 ms	fuel in
t3 (EVC)	.20 ms	pre compression
t4 (IVC)	3.62 ms	Combustion Time
T	(1.85 + 3.62) = 5.47 ms	time period

Table 9: Angular History of the Cycle

$\Theta_1 = \omega \times t1$	59.86 deg	Exhaust Angle
$\Theta_2 = \omega \times t2$	48.68 deg	$\Theta_e = \Theta_1 + \Theta_2 = 108.53 \text{ deg}$
$\Theta_3 = \omega \times t3$	13.20 deg	Inlet Angle
$\Theta_4 = \omega \times t4$	238.32 deg	$\Theta_{i} = \Theta_{2} + \Theta_{3}$ $= 61.83 \text{ deg}$

3.2 c) Simulations for RotorB with prescribed $\boldsymbol{\omega}$

The simulations so far were carried out without considering the angular velocity. The simulations are carried out with respect to the frame of motion of the rotor channel itself. Hence it is worth while to investigate the role of centrifrugal forces in the overall thermodynamics of the cycle. To investigate this a frame motion equivalent to 5000 rpm is given to the mesh. The result are summarised below

Table 10: Quantitative results for the cycle

We	17.55 J
We	587.54 J
Ws	3.35 J
Q	1.13 kJ
Н	53.45 %

Table 11: Cycle Summary from simulations

Mode (port-setting)	Time	Iteration number	Average P and T
Intialization	0	0	7 bar, 2000K
EVO	0	0	7 bar, 2000K
IVO	.89 ms	12140	.9 bar, 1200 K
EVC	1.54ms	20160	1.2 bar, 481.7 K
Ignition	1.75 ms	24270	1.55 bar, 471 K

From the comparision of the work done and efficiency number it is concluded that the centrifugal forces does not affect the overall thermodynamic cycle of the engine.

$$\omega = \text{Wnet} / \int_0^T \tau dt$$

Table 12: RPM

Ω	10,963 rpm or 1148 rad/s

Table 13: Time History of the Cycle

t1 (EVO)	.89 ms	7bar to below 1bar
t2 (IVO)	.65 ms	fuel in
t3 (EVC)	.20 ms	pre compression
t4 (IVC)	3.73 ms	Combustion Time
T	(1.74 + 3.73) = 5.47 ms	time period

Table 14: Angular History of the Cycle

$\Theta_1 = \omega \times t1$	58.54 deg	Exhaust Angle
$\Theta_2 = \omega \times t2$	42.76 deg	$\Theta_e = \Theta_1 + \Theta_2 = 101.3 \text{ deg}$
$\Theta_3 = \omega \times t3$	13.20 deg	Inlet Angle
$\Theta_4 = \omega \times t4$	245.55 deg	$\Theta_{i} = \Theta_{2} + \Theta_{3}$ $= 55.9 \text{ deg}$

But from the above tables it is infered that although the centrifugal force doesnot play a significant role in influencing the overall thermodynamic cycle, it affects the time interval during EVO, IVO, and EVC phases hence plays a role in influencing final angular shapes of the ports.

Therefore it is concluded that to obtain the final port-timings for a rotor a second simulation with correct ω is required.

3.3 Analysis of Rotor C

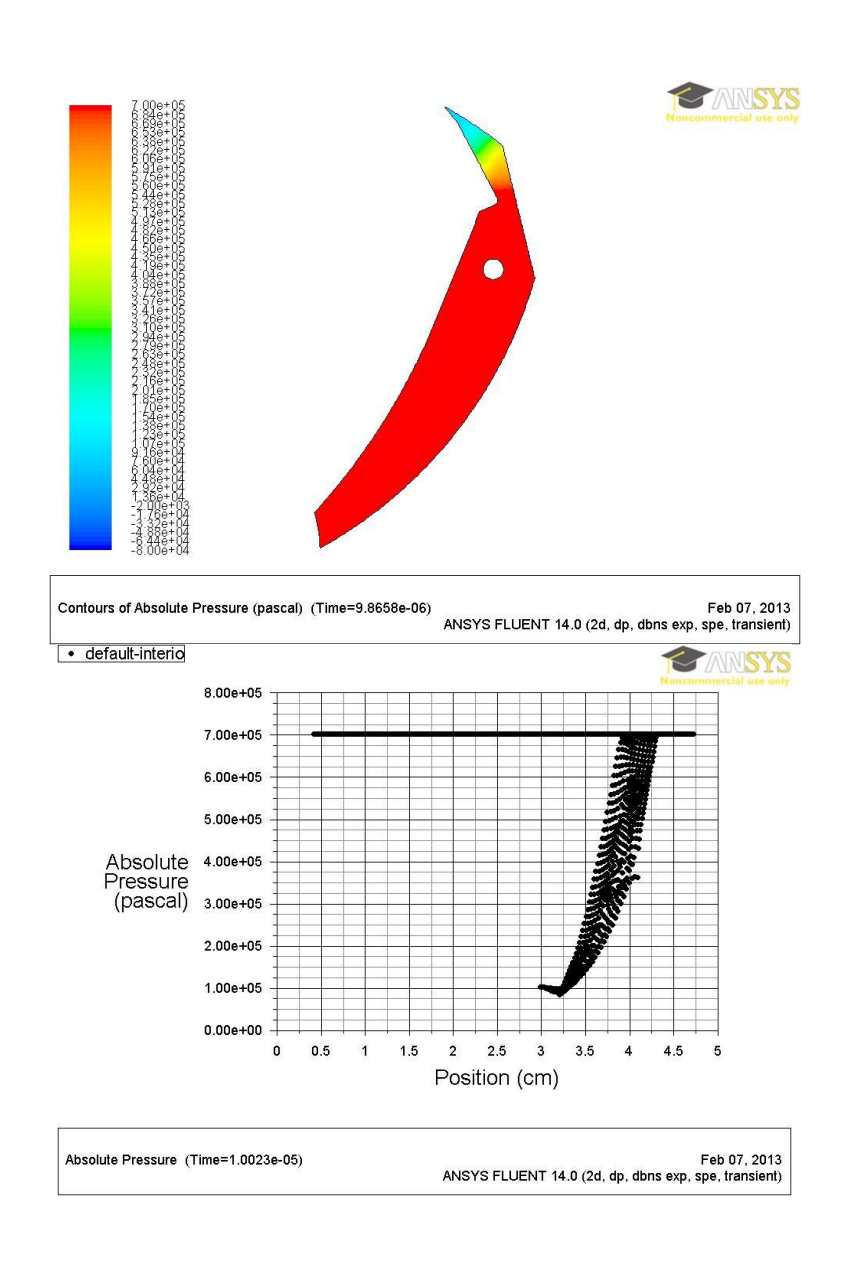


Figure 24: Sample image right before exhaust port is opened

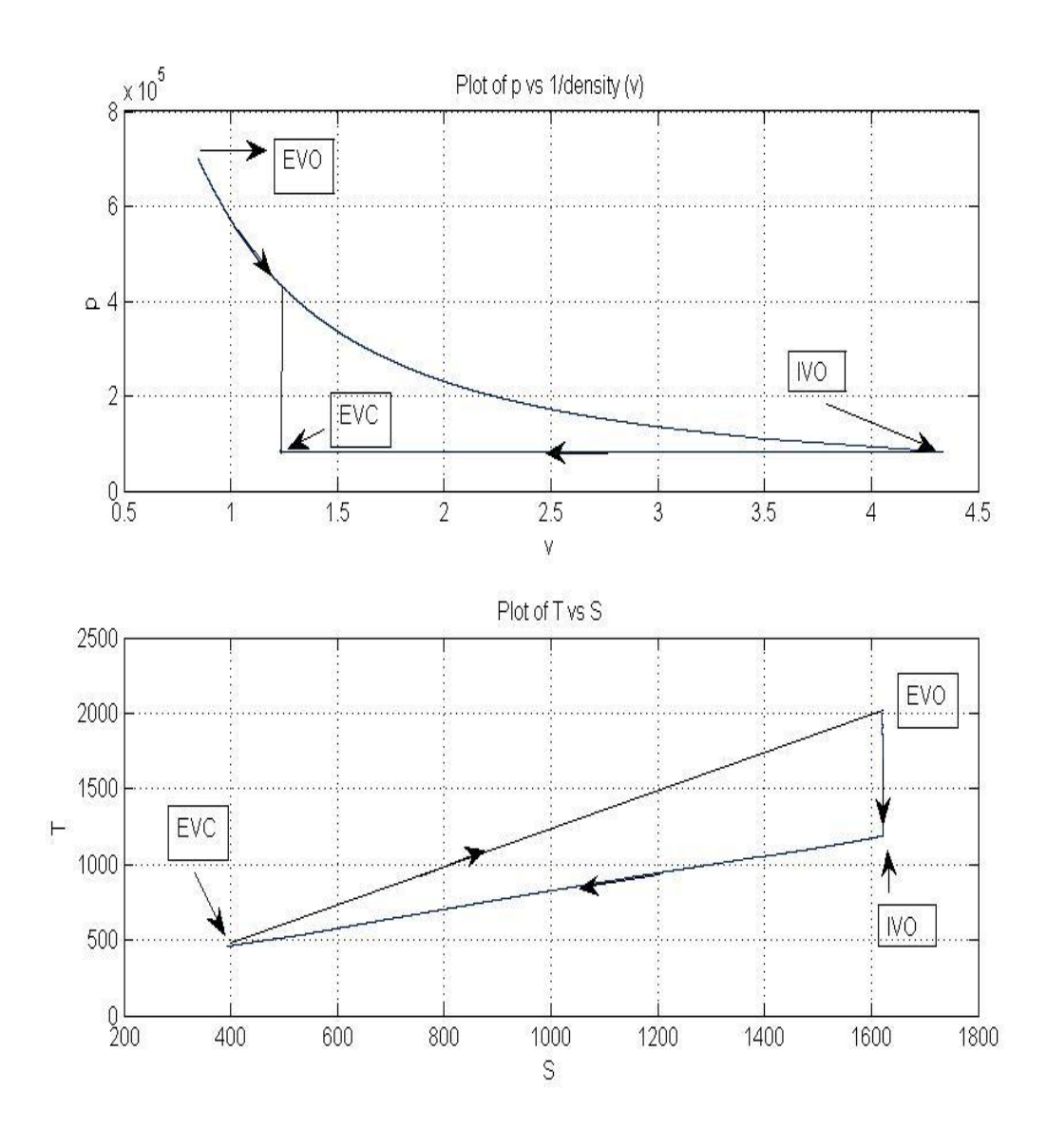


Figure 25 : P-v and T-s Diagram

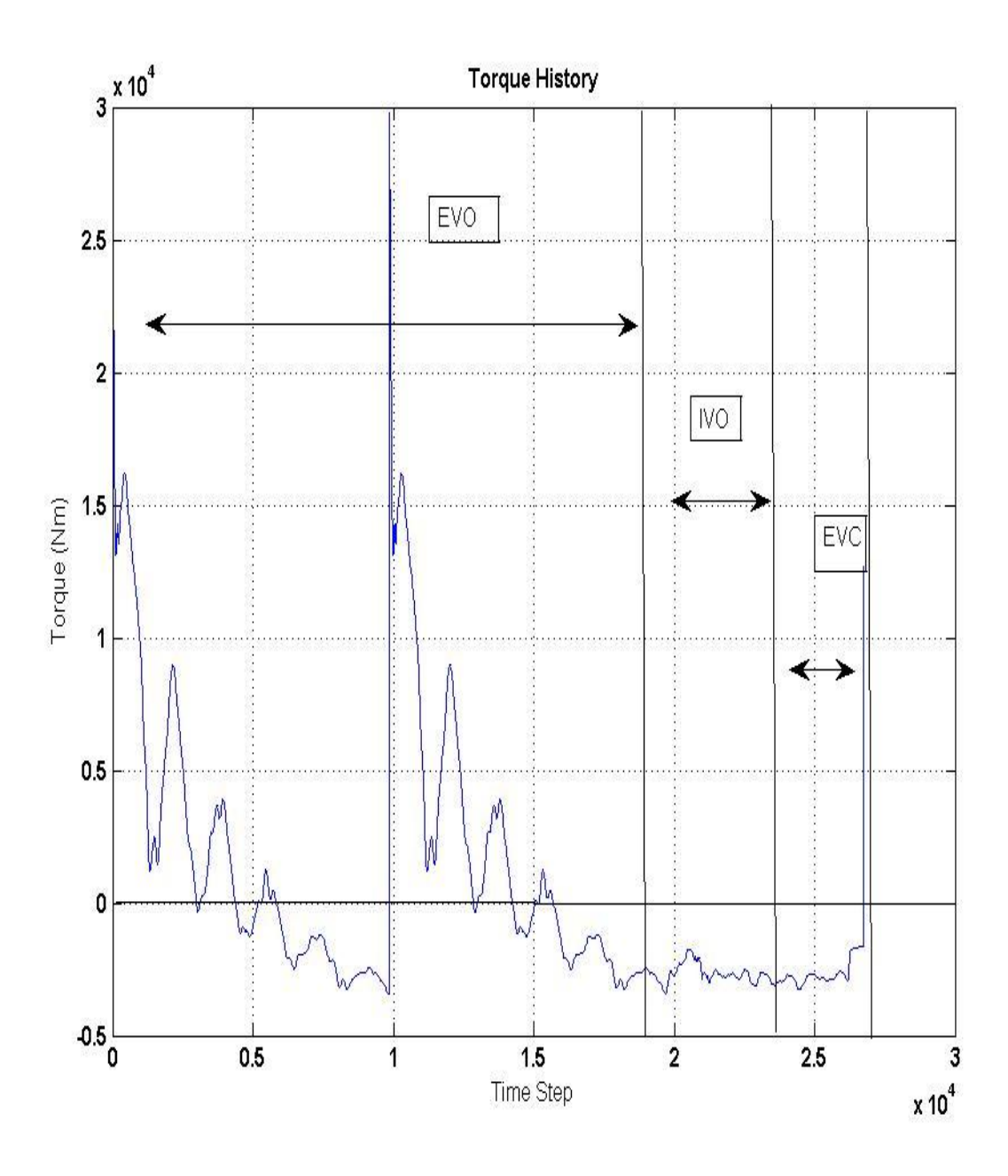


Figure 26: Torque History

3.3 a) Chronological Summary of Simulation

Table 15: Cycle Summary from simulations

Mode (port-setting)	Time	Iteration number	Average P and T
Intialization	0	0	7 bar, 2000K
EVO	0	0	7 bar, 2000K
IVO	.99 ms	13680	.9 bar, 1200 K
EVC	1.52 ms	20680	1.2 bar, 481.7 K
Ignition	1.87 ms	25959	1.55 bar, 471 K

Table 16 : Quantitative results for the cycle

Wc	0.0032 J
We	1274 J
Ws	-500.20 J
Q	1.70 kJ
Н	46.9 %

As calculated above the rotational speed is determinjed as :-

$$\omega = \operatorname{Wnet} / \int_0^T \tau dt$$

Table 17: RPM

Ω	87933 rpm or 920.83 rad/s

Table 18: Time History of the Cycle

t1 (EVO)	.99 ms	7bar to below 1bar
t2 (IVO)	.53 ms	fuel in
t3 (EVC)	.35 ms	pre compression
t4 (IVC)	4.95 ms	Combustion Time
T	(1.87+4.95) =6.82 ms	time period

Table 19: Angular History of the Cycle

$\Theta_1 = \omega \times t1$	52.2 deg	Exhaust Angle
$\Theta_2 = \omega \times t2$	28.0deg	$\Theta_e = \Theta_1 + \Theta_2 = 80.19 \text{ deg}$
$\Theta_3 = \omega \times t3$	18.5 deg	Inlet Angle
$\Theta_4 = \omega \times t4$	261.3 deg	$\Theta_{i} = \Theta_{2} + \Theta_{3}$ $= 46.43 \text{ deg}$

3.4 Comparsion of Rotor A,B and \boldsymbol{C}

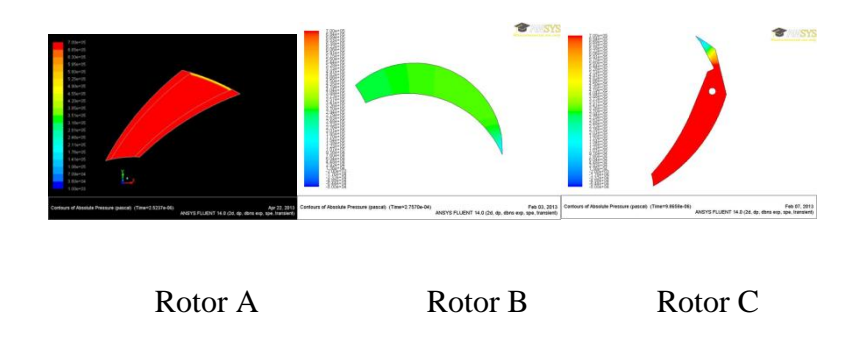


Figure 27 : Comparison of Rotor A,B and \boldsymbol{C}

Table 20: Comparison of the three rotors

	Rotor A	Rotor B	Rotor C
Wc	-79.34 J	17.55 J	.0032 J
We	379.65 J	587.4 J	1274 J
Ws	24.86 J	3.35 J	-500.2 J
Wnet	325.13 J	608.3 J	773.8 J
Q	949.26 J	1.108 kJ	1.7 kJ
η	34.26 %	54.45 %	46.9 %
Power	37.81 kw	110.6 kw	113.5 kw

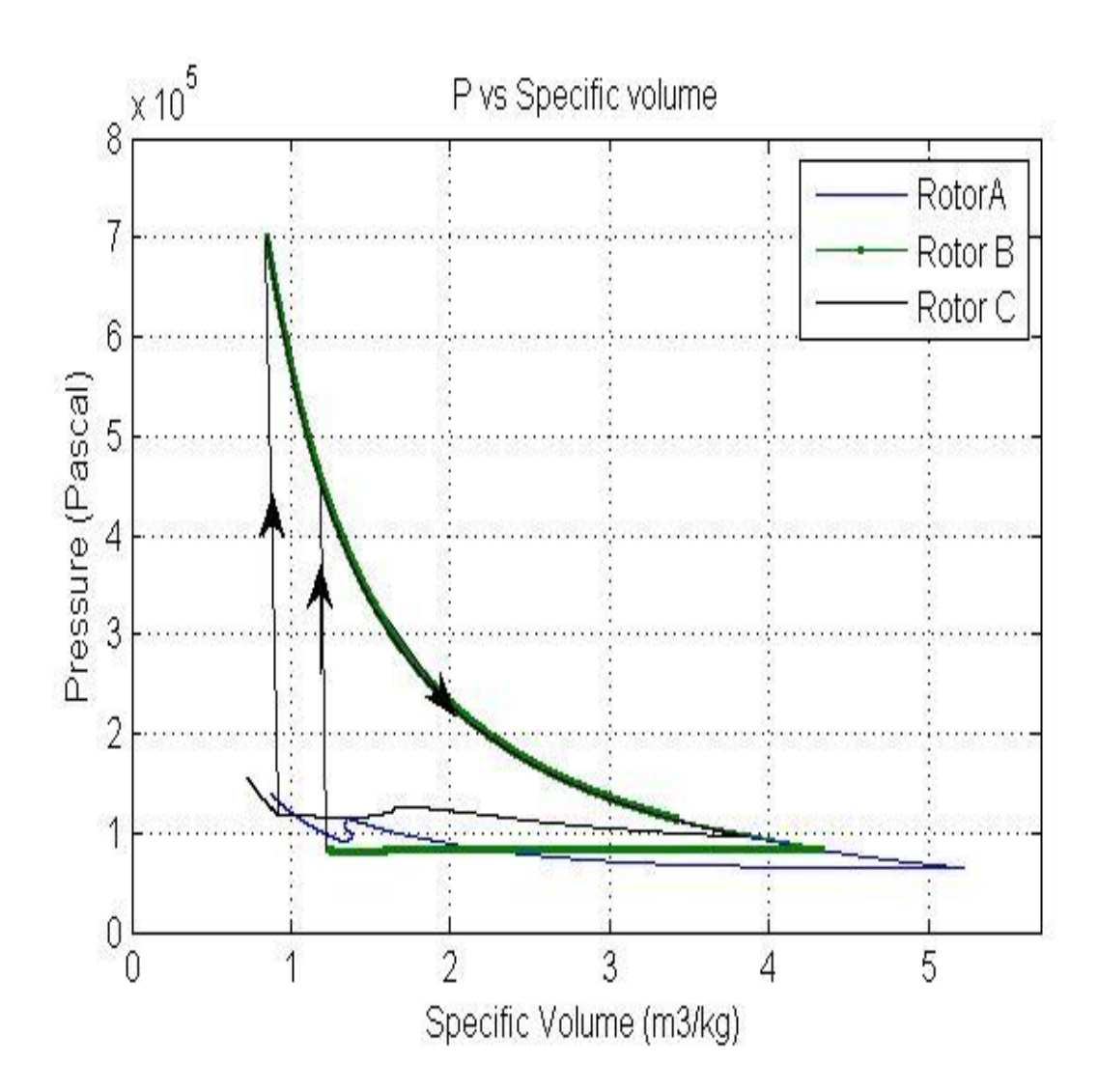


Figure 28 : Comparison of P-v diagram

3.4 a) Discussion

- 1. Rotor A is least efficient and has least power output. This is owing to the fact that mass flow rate at outlet is not restricted hence lot of mass goes out at a higher total enthalpy without exchanging energy. This is illustrated from following figures.
- **2.** Rotor C has superior torque output owing to the convergig-diverging shape of outlet. Though the complicated channel shape results in alomost zero precompression
- **3.** Rotor B is most efficient, although the power output is low comparative to rotor C but owing to lesser torque output it will result in more losses in real world operations.
- **4.** The power output can be increased if the gases exiting at outlet can further be expanded via external turbines.

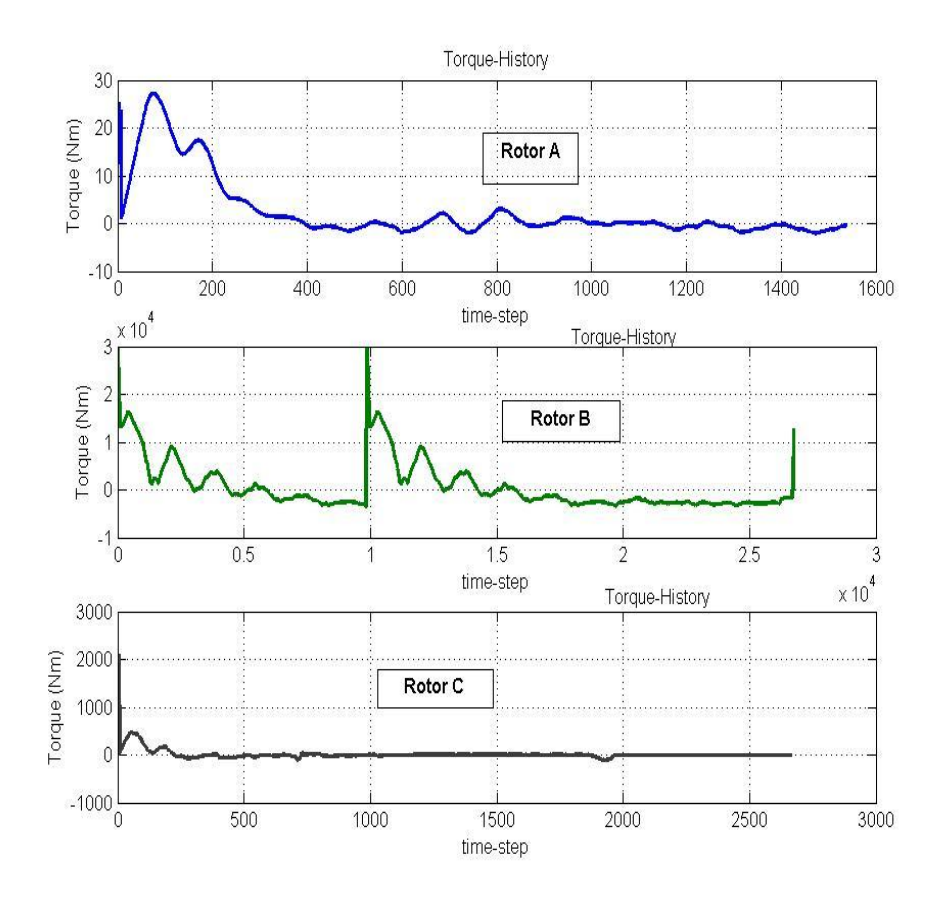


Figure 29: Torque-History of all three rotors

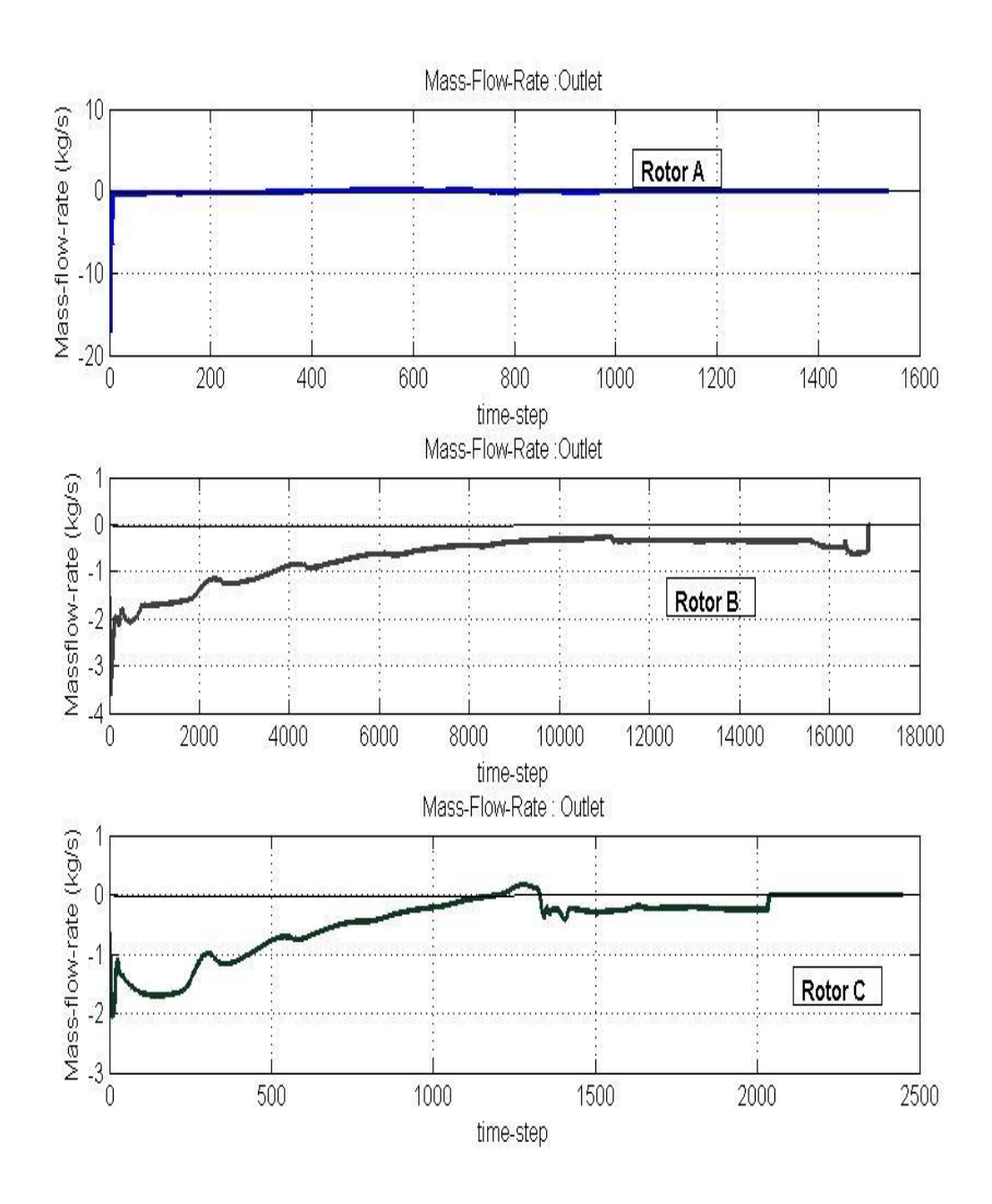


Figure 30: Mass-flow-rate at the outlet of the rotors.

3.5 Modified Rotor A

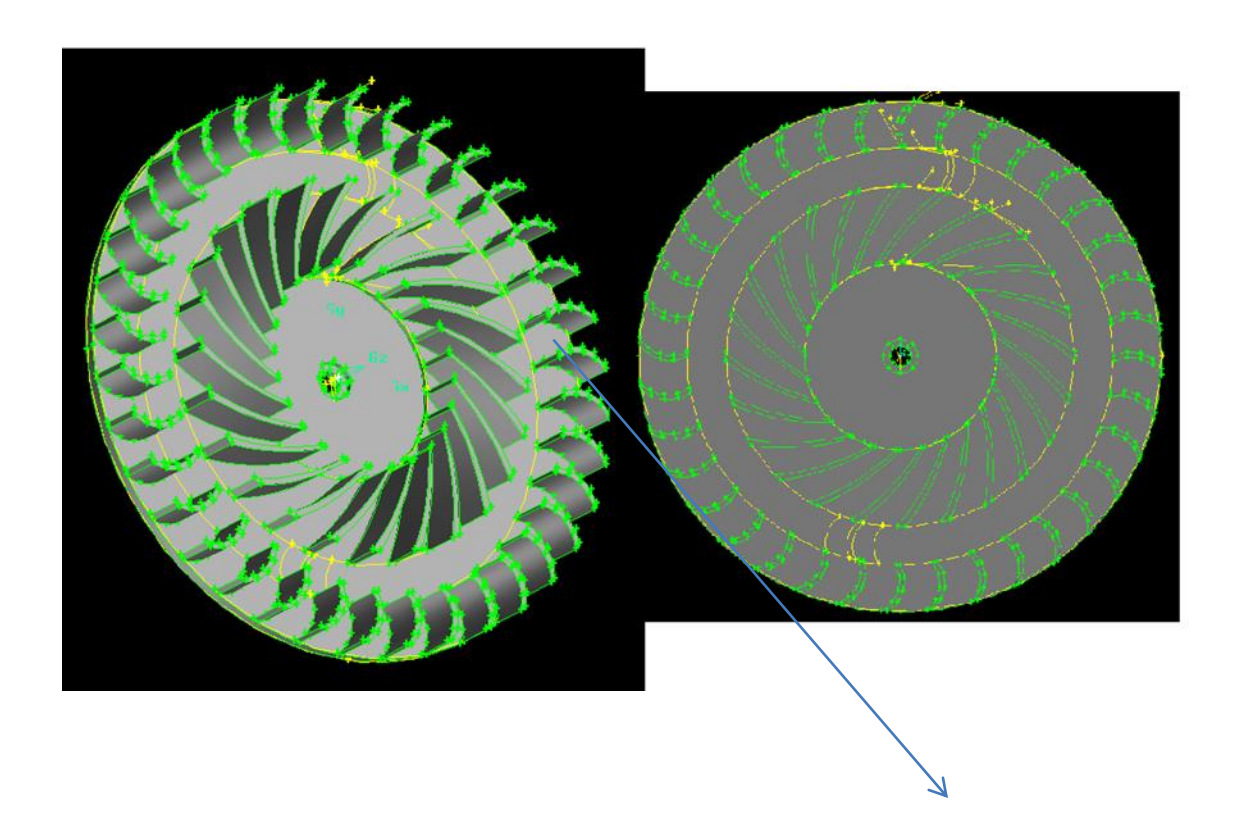


Figure 31: 3D view of Rotor A- with external row of turbine

To simulate the complete cycle for one given channel a simplified passage of rotor channel guide vane and turbine channel is meshed. The figure below depicts the simplified 2D mesh.

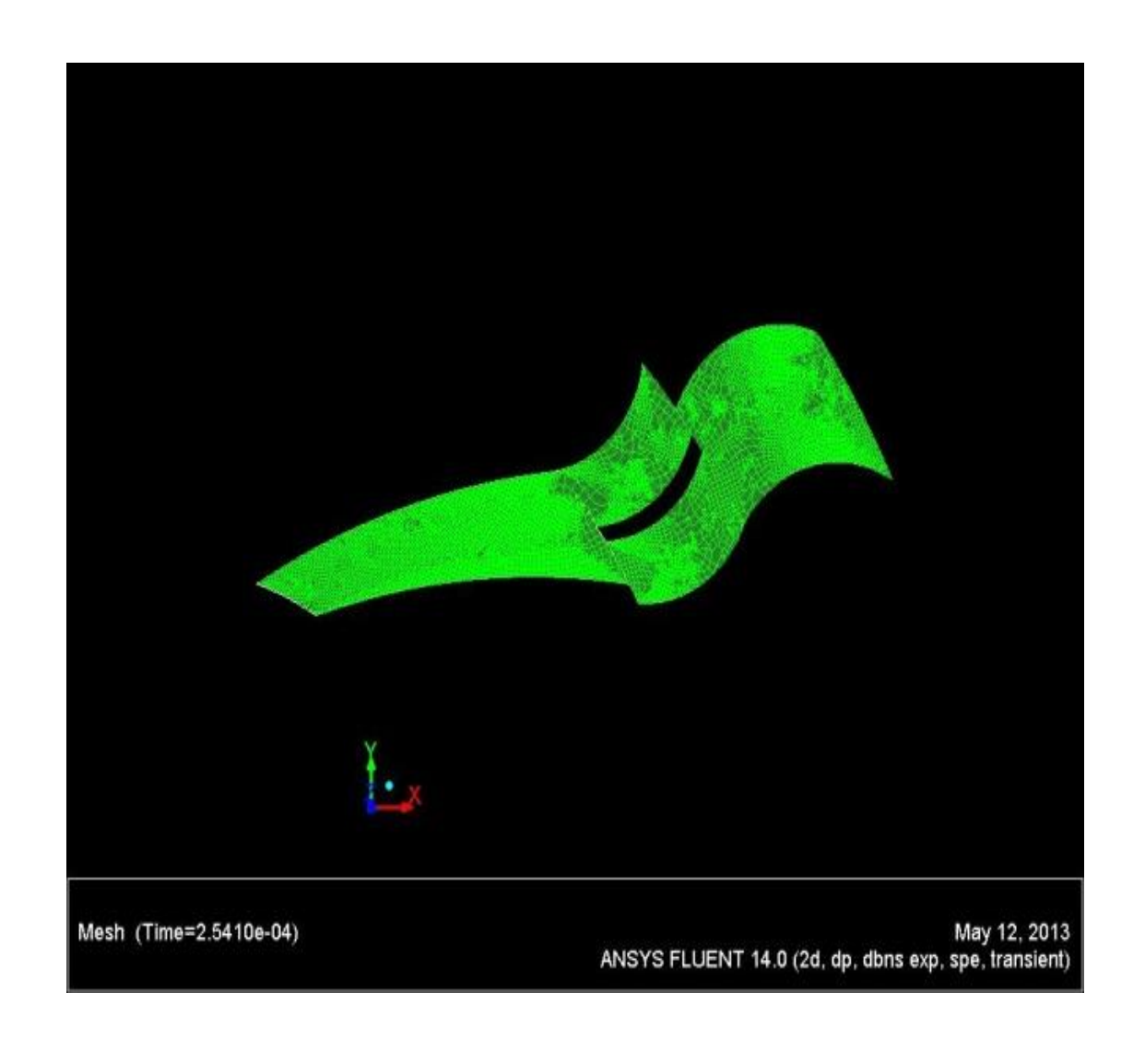


Figure 32: Modified Rotor Channel with external channel

3.5 a) Simulation Summary

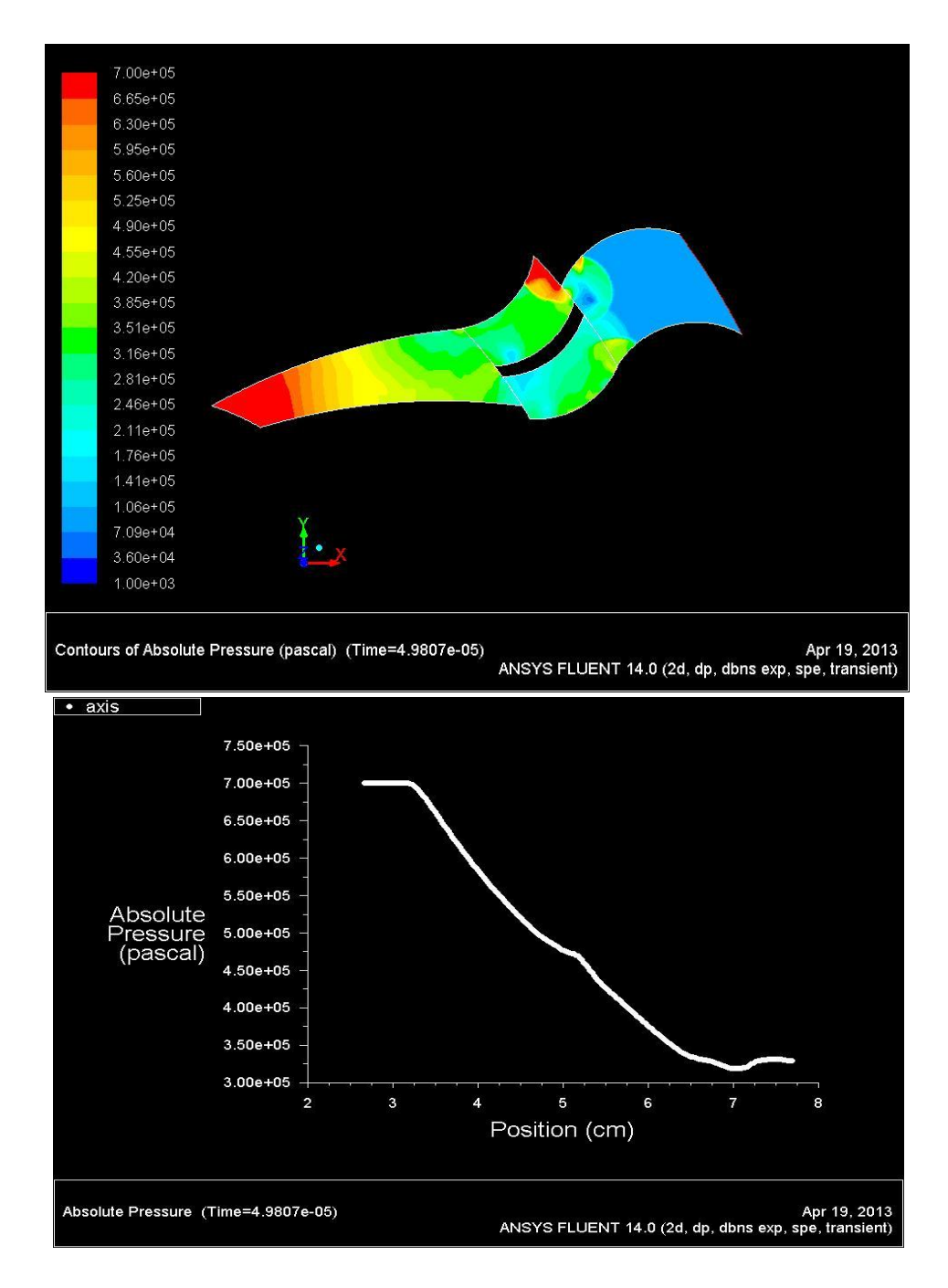


Figure 33: Sample image from simulations, depicting pressure contour after the outlet port is opened

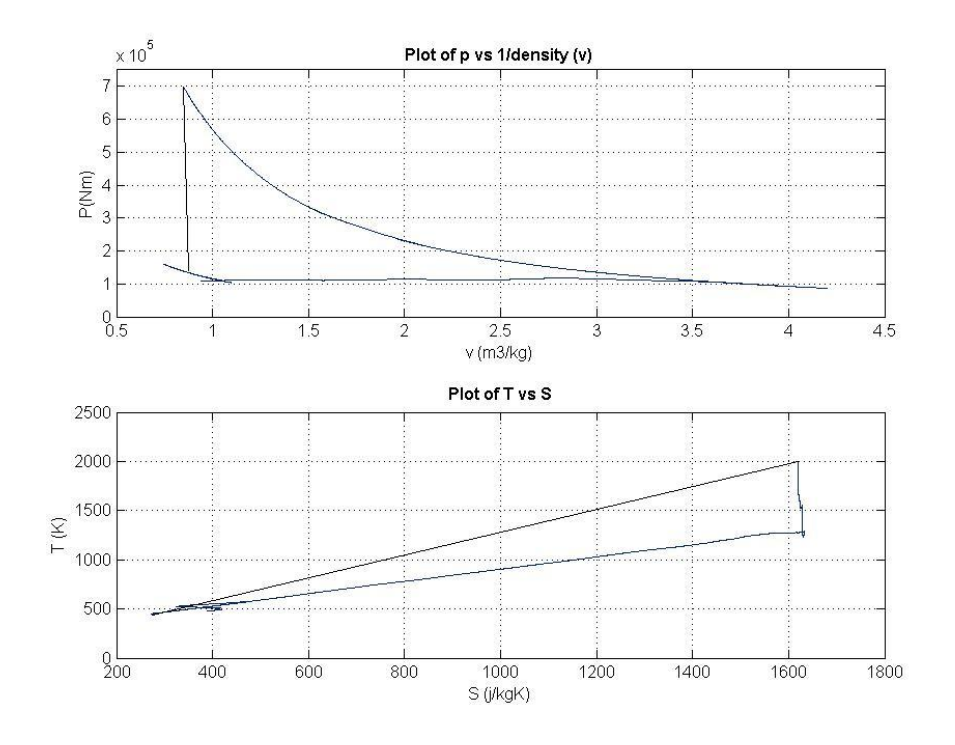


Figure 34: P-v ans T-s Diagram

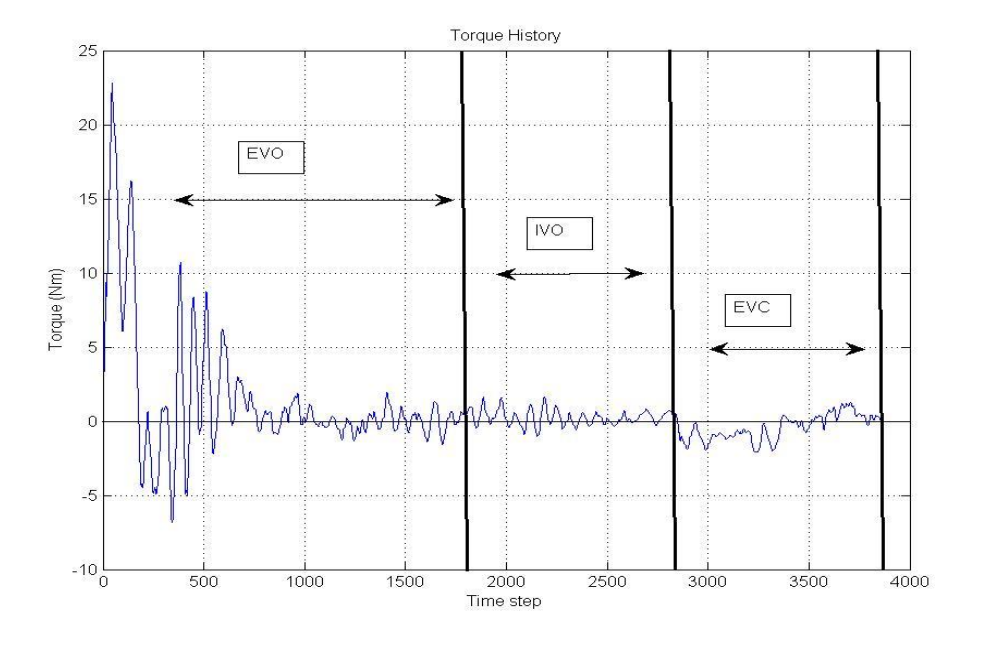


Figure 35 : Torque History

3.5 b) Chronological Summary of Simulation

Table 21 : Cycle Summary from simulations

Mode (port-setting)	Time	Iteration number	Average P and T
Intialization	0	0	7 bar, 2000K
EVO	0	0	7 bar, 2000K
IVO	.532 ms	17500	.9 bar, 1200 K
EVC	1.12 ms	28370	1.2 bar, 481.7 K
Ignition	1.7 ms	38570	1.55 bar, 471 K

Table 22: Quantitative results for the cycle

Wc	-97.60 J
We	1223 J
Ws	-70102J
Q	950 kJ
Н	37.31 %

In addition work done by external turbine = mass flow rate at outlet of rotor *(total enthalpy at rotor outlet-total enthalpy at turbine outlet) = 58.34 J. This gives net work output of **412.79** J.

Hence the effective efficiency is 43.45 %

As calculated above the rotational speed is determinized as :- ω = Wnet $/\int_0^T \tau dt$

Table 23: RPM

Ω	17000 rpm
	1780.24 rad/s

Table 24: Time History of the Cycle

t1 (EVO)	.99 ms	7bar to below 1bar
t2 (IVO)	.53 ms	fuel in
t3 (EVC)	.35 ms	pre compression
t4 (IVC)	3.53 ms	Combustion Time
T	3.53 ms	time period

Table 25: Angular History of the Cycle

$\Theta_1 = \omega \times t1$	100.98 deg	Exhaust Angle
$\Theta_2 = \omega \times t2$	54.1 deg	$\Theta_e = \Theta_1 + \Theta_2 = 155.04$
$\Theta_3 = \omega \times t3$	35.7 deg	Inlet Angle
$\Theta_4 = \omega \times t4$	360 deg	$\Theta_{i} = \Theta_{2} + \Theta_{3}$ =89.8 deg

3.5 c) Comparison of Rotor A vs Modified Rotor A

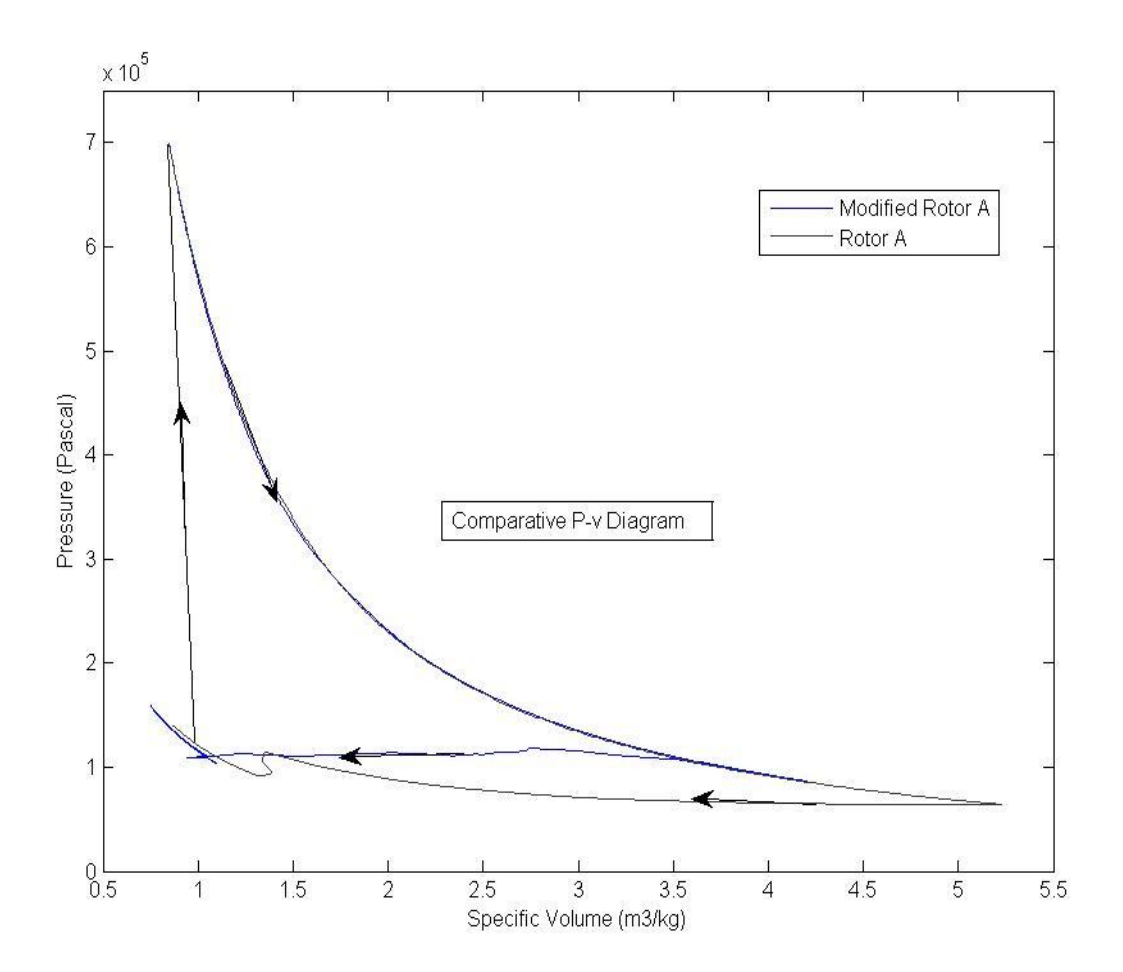


Figure 36 : Comparitive P-v diagram

- 1. Rotor A when operated with an external turbine in tandem results in higher efficiency but the torque output is still low, hence the operating RPM is still high (17000).
- **2.** Modified rotor A has better pre-compression ratio (1.5 against 1.33). Though the increase in precompression is not significantly high
- **3.** We conclude that because of the poor torque output of the rotor A, it is not a feasible design even if topped up with an external turbine.
- **4.** Multiple rows of external turbine is required to enhance the torque output of Rotor A.

Chapter 4 : Conclusion and Future work

- Converging shape of rotor channel enhances thermal efficiency by creating stronger compression waves.
- Torque output is more when a C-D outlet shape is chosen, this weakens the compression wave.
- Therefore a rotor channel shape is a subject of optimization by balancing this two competing phenomena
- Current methodology is a handy tool in comparing different rotor shapes.
- The methodology can be further refined by including gradual valve opening limitations,
 effect of viscosity, heat losses across non adiabatic wall, and integrating simulation with
 combustion models
- Practical Designs of wave rotor based machines are badly impacted by leakage.

REFERENCES

REFERENCES

- [1] Anderson, John, 1995, Computational Fluid Dynamics: the Basics with Applications, McGraw-Hill Science/Engineering/Math
- [2] Akbari, P., Nalim, M. R., Mueller, N., "A Review of Wave Rotor Technology and Its Applications," ASME Journal of Engineering for Gas Turbines and Power, October 2006, Vol. 128, pp. 717-735.
- [3] Snyder, P., Alparslan, B., and Nalim, M. R., "Gas Dynamic Analysis of the Constant Volume Combustor, A Novel Detonation Cycle," AIAA Paper 2002-4069, 2002.
- [4] Paxson D. E.,1996, "Numerical Simulation of Dynamic Wave Rotor performance," AIAA Journal of Propulsion and Power, Vol. 12, No. 5, pp.949-957, (also, NASA TM 106997).
- [5] Paxson D. E., 1995, "A Numerical Model for Dynamic Wave Rotor Analysis," AIAA Paper 95-2800. Also NASA TM-106997.
- [6] Akbari, P. and Nalim, M. R., "Review of Recent Developments in Wave Rotor Combustion Technology." Journal of Propulsion and Power, Vol. 25, No. 4, pp 833-844, July–August 2009.
- [7] Iancu. F, Piechna. J, Dempsey. E, and Müller. N, "The Ultra-Micro Wave Rotor Research at Michigan State University, second International Symposium on Innovative Aerial/Space Flyer Systems, The University of Tokyo, 2005, pp 65–70.